Influence of soil-structure interaction on the fragility curves of medium-height moment resisting frames and thin-walled buildings located in Bogotá, Colombia

Angie Viviana Osorio Castellanos

Universidad de La Sabana

Faculty of Engineering

2023

Influence of soil-structure interaction on the fragility curves of medium-height moment resisting frames and thin-walled buildings located in Bogotá, Colombia.

A dissertation submitted in partial fulfilment of the requirements for the degree of:
Master of Process Design and Management

Logistics Systems Emphasis

Angie Viviana Osorio Castellanos

Advisor: Orlando Daniel Arroyo Amell, PhD.
Universidad de La Sabana.

Co-advisors: Wilmer Julián Carrillo León, PhD.
Universidad Militar Nueva Granada.
Miguel Enrique Sarmiento Díaz, Msc.
Universidad de La Sabana.

Universidad de La Sabana
2023

Dedication

This work is dedicated in first place to God who gave me the strength to face the challenges during its elaboration. To my beloved parents who were always supportive and were always by my side when things got difficult. To my little brother who always cheered me up with his paintings and hugs. To my friends for making this path more joyful.

Acknowledgments

Table of Contents

List of Figures

List of Tables

Abstract

Nowadays, Bogotá's population accounts for 15% of the total Colombian population. The population influx the city has experienced has increased the construction of buildings in the past decades. Mid-rise buildings represent over 24% from the total building stock of the city and have been constructed mainly using reinforced concrete (RC) structural systems such as moment resisting frames and thin walls. The vulnerability of such systems has been studied and documented through fragility curves that are constructed based on structural analysis results and laboratory tests. The common practice among practicing engineers to carry on the structural analysis is assuming a fixed base building, which means that the structure is founded on rock or soils with a considerable strength, neglecting the displacements that can be produced due to the presence of the foundation and the soil beneath. Such assumption may lead to inaccurate results in the case of Bogotá where an important percentage of the foundation subgrade are soft clays with high compressibility and low bearing capacity. This type of soils has been proved to affect considerably the seismic performance of buildings during earthquakes. Therefore, this research studied the influence of the soil-structure interaction on structural analysis of RC moment resisting frames and thin walls mid-rise buildings founded on the soft soils area of Bogotá by means of dynamic analysis using OpenSees. Results showed that considering both the foundation and the soil, the stiffness and the system ductility reduce, and the fragility compared to the common fixed base approach increases

1 Chapter I: Overview

1.1 Introduction

The behavior of a structure when subjected to seismic loads can be described through parameters such as roof and inter-story drifts, floor accelerations, etc., which are obtained from structural analyses conducted by means of the elaboration of structural models. The most used parameter is the inter-story drift, which is a translational displacement between two consecutive stories [1] and is often related to the damage that the structure may suffer during a seismic event. In the past decades, the damage that a structure experiences due to an earthquake has been assessed by the generation of fragility curves, which has become a common approach among researchers and some practicing engineers since the importance of the safety level of structures has increased. Such curves correlate the probability of a damage level to be reached or exceeded (i.e., slight, moderate, extensive or collapse) given an intensity measure [2]. The fragility curves can be computed by means of field observations, laboratory tests or numerical analyses.

However, the study of the fragility of a building entails some simplifications and assumptions; one of the most used since the 90s is that the building model base is fixed, which has simplified the numerical calculations and has proven to be a good approach to estimate the seismic performance of structures founded on firm soils [3]. Nevertheless, it has been documented that neglecting the foundation-soil system in the analyses may entail an underestimation of the fragility of a structure, especially when the stiffness of the superstructure is higher than that of the foundation and the soil. In such cases, the structural damage not only depends on the superstructure, but also on the behavior of the soil beneath [4], [5]. The study of the complete system (i.e., superstructure, foundation and soil) is known as soil-structure interaction (SSI), which

aims at assessing the stresses and strains that occur in both, the soil and the structure due the difference between the material stiffnesses [6].

SSI can be studied for static and dynamic loads. In the former case, the compatibility of strains between the structure, the foundation, and the soil along the service life of the structure is evaluated [7]. Such strains are the response of the soil to the presence of the structure, which affects the mechanical properties of the material. In the dynamic case, two aspects are studied. The first one is the change in the ground motion due to the presence of the structure during a seismic event (kinematic interaction) and the second one consists of determine the structural response when the modified motion is considered (inertial interaction) [8].

There are two main approaches to incorporate SSI in the structural modeling. The first one is called the direct method and consists of using finite elements to model the soil and the structure. In the process, interface elements to join the soil and the foundation are created, and the analyst ensures that the soil modeling is properly extended around and under the foundation to consider the properties of the site. In practice, the direct method is generally used in large-scale projects such as nuclear power plants or large infrastructures such as bridges, tunnels, etc. [9] as such structures requires a more profound analysis due to its complexity. The second method is known as the substructure method, in which the structure and the soil are studied as two separated systems. The foundation behavior is represented by dampers and springs that are computed using impedance functions [10]. The impedance functions consist of complex numbers, where the real part represents the stiffness, and the imaginary part represents the damping. The impedance equation that describes the behavior can be expressed using Equation 1.1.

$$S = K + i\omega C \hspace{3cm} \text{Equation 1.1}$$

Where: S represents the impedance function of the soil-foundation system, K represents the stiffness of the system, C represents the damping coefficient of the system, ω represents the angular frequency of the seismic solicitation and i represents the imaginary unit.

The impedance functions can be computed using numerical methods. Transformed integral [11], the boundary element [12], dynamic finite element [13] and Novak's methods [14] are commonly used for analysis and the last one has its applications on piles and pile groups analyses. The computation method selection involves an adequate knowledge of the soil-foundation system and ground motion characteristics (i.e., embedment, soil profile, vibration mode and frequency of excitation).

Additionally, modeling SSI can be addressed linear or nonlinearly, depending on the characteristics defined for the elements used. Generally, studies consider nonlinearity in one of the two components of the interaction (i.e., structure or soil) [15]. Regarding soil modeling, existing literature describes three primary methods: continuum models, Beam on Nonlinear Winkler foundation (BNLWF), and plasticity-based macro-elements [16]. The SSI on deep and shallow foundations is usually modeled with discrete elements (i.e., vertical and horizontal springs) [17], whose stiffness is computed from equations proposed by Gazetas [18], Vesic, Bowles [19], among others. Several studies conducted by researchers have demonstrated that the inclusion of SSI in the analysis of the seismic performance of buildings result in changes of structural properties such as the fundamental period, the stories displacements and ductility.

1.2 Justification

The experience with past earthquakes has demonstrated that the structural behavior can undergo changes due to site effects and SSI. In the earthquake of Mexico City, 1985 (Mw 8.1), the

soil played a key role in building collapse. For instance, during the earthquake of Mexico City, accelerograms located in the valley of Mexico reported different amplitudes and durations for the same event. The accelerometers located in the lake area recorded greater amplitudes in the movement and longer durations than those reported in other locations. It was found that the soft soils amplified the seismic waves leading to resonance, which mainly affected tall buildings [20]. Given the unique geotechnical and geological conditions of Mexico City, practicing engineers along with researchers have carried out exhaustive studies aimed at improving the seismic performance of the structures designed for the city specially for the lake zone [21]–[26].

In South America, there is a city that holds similar geological characteristics to Mexico City. Such city is Bogotá, the capital of Colombia, whereby a microzonation study carried out by Los Andes University together with INGEOMINAS (today the Colombian Geological Service) divided the city into five main zones: rock (roca), foothill (piedemonte), stiff soils (suelos duros), soft soils (arcilla blanda) and river and wetland (rondas de ríos y humedales) as depicted in Figure *1.1* [27].

Despite the antecedents observed in Mexico City during the seismic events, the SSI effect on the seismic performance of structures constructed in Bogotá is not well documented, as the fragility analyses conducted for buildings with different structural typologies located in the city (i.e., Moment resisting frames, Reinforced and Unreinforced Mansory and RC thin walls) [28]–[31] assumed the fixed base approach. In fact, the only research work known by the author where SSI effect is studied is the master thesis of Bahamon [32] who conducted static nonlinear analyses (pushover) for a 10-stories building RC-MRF with piles in the lacustrine soils of Bogotá. He pointed out that SSI enhanced the ductility of the system, which reflected in higher displacements than the observed in the fixed base. Given the lack of structural analyses of buildings that include

4

SSI effects and the particular characteristics of the subgrade of Bogotá, this research work aims at answering the following question:

How does the SSI affect the fragility curves of mid-rise RC moment resisting frames and thin-walled buildings founded on piles in soft soils of Bogotá?
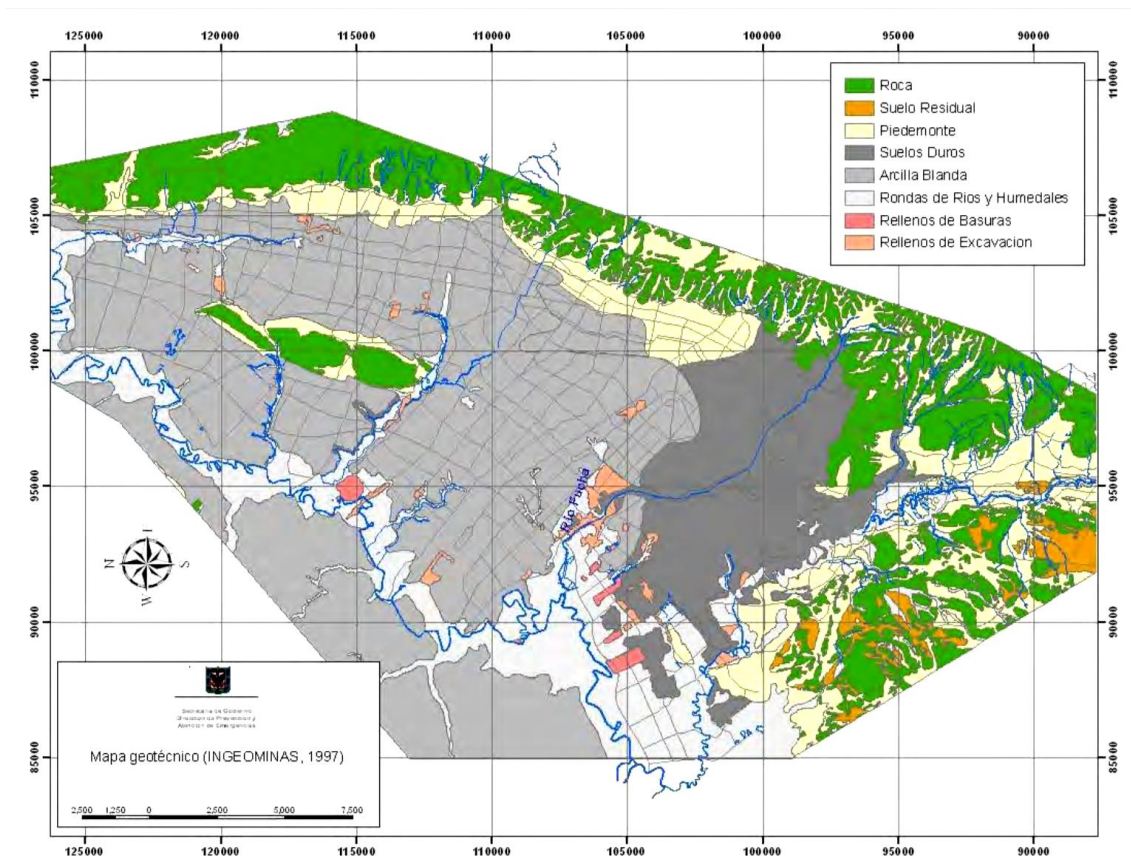
Figure 1.1 Bogotá microzonation. Source: Fondo de Prevención y Atención de Emergencia (FOPAE) [33]

1.3 State of the art

In the first reports of SSI, it was considered beneficial [34] due to the reduction of internal forces and drifts observed in the buildings as a result of the increment in the soil flexibility; therefore, the fixed base approach was deemed as more conservative. However, such behavior is not generalized for all types of buildings nor soils, since observations made in certain seismic

5

environments and soils led to realize that the increase in structure characteristics such as the fundamental period is detrimental, especially for flexible structures [35]. Several authors [36]–[48] have studied and reported the seismic performance of buildings including SSI using different approaches. Soltani-Azar [36] and Bandyopadhyay *et al.* [37] used site-specific spectra that included the nonlinearities in soil to construct artificial ground motions to assess the performance of mid-rise and tall RC structures via dynamic analyses. Both studies reported that the structures undergo an increment in the vulnerability.

Kraus and Džakić [38] studied the SSI effect on the seismic behavior of RC frames designed following the Eurocode prescriptions. They compared the results for a building with fixed base and flexible base with the soil modeled as Winkler springs and as a half-space. The results showed that the models that included the soil, exhibited higher values of story drifts and contrary to what was thought, the internal forces of the structural elements did not diminish in mid-rise buildings.

Bakhshi and Ansari [39] used fragility curves to define the vulnerability of two RC MRF buildings; one of 12 and the other of 24 stories founded in C and D type soils (classified in accordance with National Earthquake Hazards Reduction Program, NEHRP). The building models were developed using OpenSees [49] and included the structural uncertainties by using Monte Carlo simulations to define the material properties. The uncertainty in the soil properties was neglected and the SSI was modeled using the substructure approach with the cone model and equivalent springs and dashpots. The results showed that the exceedance probability of damage states was increased when SSI was included in structural analysis, especially for D-type soils. Similarly, Akhoondi and Behnamfar [40], reported that the collapse probability of Steel MRF buildings rise between 11% and 21% and between 3% and 13% for 4- and 12- stories buildings,

respectively, when the SSI is considered. Anvarsamarin *et al*. [41] generated collapse fragility curves for 3D RC MRF buildings with sallow foundation considering SSI using the cone model. Their results indicated that the mean value of the intensity measure of the fragility analysis (θ) reduced by 4.9%, 22.3% and 23.0% for 6-, 12- and 18- story buildings, respectively, which means that the buildings were more likely to reach a certain damage state at lower intensity measures. Likewise, Oz *et al*. [42] found that SSI increased the displacement in low and mid-rise RC buildings when the soil characteristics considered described soft behavior, compared to the rigid approach modeled as fixed base.

Tahghighi and Mohammadi [43] studied the SSI in RC frames shallowly founded by constructing models in OpenSees finite-element framework based on nonlinear Winker method for three types of soils. They found that the performance level of mid-rise buildings on soft sites increases when compared to the rigid approach. This means that a specified performance level (i.e., Immediate Occupancy, Life Safety and Collapse Prevention), was obtained at a larger displacement when the SSI is considered. Additionally, the authors pointed out that the inter-story drifts increased along with the number of stories of the building. Similarly, Pitilakis and Petrtidis [44] assessed the vulnerability of a building block in Thessaloniki, Greece, which consisted of ten RC MRF and eight Dual system buildings for three foundation cases: rigid, rigid including site amplification effects, and flexible foundation with BNLWF. The findings showed that the nonlinear soil behavior along with SSI effects detriments the vulnerability of the buildings block, leading to higher damage, therefore higher economic losses. Requena-Garcia-Cruz *et al.* [45] also evaluated the seismic performance of mid-rise RC structures shallowly founded in Lisbon, using BNLWF and the direct method in OpenSees. The results led to conclude that the increment in soil flexibility translates into higher structural periods and structural damages, which means that

neglecting SSI effects may lead to an overestimation of the initial stiffness of the structure and its capacity. Additionally, it was noted that the seismic behavior obtained with the BNLWF approach was as accurate as the direct modelling.

Kechidi *et al*. [46] proposed a practical approach for modelling SSI in OpenSees based on the monkey-tail fundamental lumped parameter developed by Wolf [50], which consists of a range of springs and dashpots-masses with lumped values that represent the stiffness. This approach articulates the use of MATLAB and OpenSees software to calculate and implement SSI in the execution of nonlinear analyses. The application of the method was done in two 5-story RC MRF buildings and the results leaded to point that neglecting SSI entails a relevant underestimation of the seismic response observed in the displacements obtained for the lower stories, which were larger than those observed in the rigid base model.

Carbonari *et al*. [47], [48] studied the effect that SSI exerts in the fragility of a coupled wall-frame system on pile foundations. The structure modeling was conducted linear and nonlinearly, and three soil conditions were assessed. Their findings support the importance of the inclusion of SSI in seismic analyses as major lateral deformability was observed leading to earlier damage in structural and non-structural elements.

In Latin America, fragility studies are found the literature for residential buildings such as the study of Villar-Vega [29]. For Colombia, Acevedo *et al.* [28] calculated fragility curves for the three main cities of the country (i.e., Bogotá, Cali and Medellín). Regarding vulnerability evaluation using fragility curves in Bogotá, the thesis of Melendez and Santisteban [30] describes fragility curves of the San Ignacio Hospital before and after its restoration works. However, the mentioned studies did not consider the SSI effect.

Although research has been conducted in fragility analysis considering SSI around the world, most of the studies were addressed in buildings shallowly founded (mainly MRF and no thin-walled structures). In addition, no reports in the matter were found in Bogotá. Therefore, a gap of knowledge in the study of SSI for MRF and thin-walled buildings founded on piles is identified [15]. Shedding some light in the matter, this work focuses in studying the effect that SSI has on the seismic performance of mid-rise RC moment resisting frames and thin walls buildings founded in the soft soils of Bogotá, Colombia.

1.4   Objectives

1.4.1   General Objective

Evaluate the influence of the soil-structure interaction in the fragility curves of mid-rise buildings with reinforced concrete moment resisting frames and thin walls reinforced with welded-wire mesh, with deep foundations in soft soils of Bogotá.

1.4.2   Specific Objectives

- ✓ Apply incremental dynamic analysis to reinforced concrete moment resisting frames and thin walls with and without soil-structure interaction.
- ✓ Calculate fragility curves for light, moderate, extensive and collapse damage states for both structural systems.
- ✓ Estimate the effect of the soil-structure interaction on the fragility curves of both structural systems.

2 Chapter II: Seismic Performance of Mid-Rise Reinforced Concrete Buildings Designed for Intermediate Seismic Hazard Zones in Colombia

2.1 Introduction

Colombia is located within one of the most active seismic zones on earth since its territory lies in the area where the Nazca and Caribbean plates converge against the South American plate, leading to divide the country into low, medium, and high seismic hazard zones [28]; 87% of the total Colombian population live in these last two [51]. Efforts to mitigate seismic risk are necessary, and to achieve this, the design of the structures is regulated by earthquake-resistant code provisions that result from analytical, and experimental research and are commonly updated considering the documented experience of past earthquakes [52]. Pioneer building codes did not incorporate significant requirements for earthquake-resistant design because their main goal was to achieve acceptable performance for gravity loads [53]. Such criteria showed to be inappropriate in seismic active zones leading to significant structural damage during seismic events [54] since buildings did not have sufficient strength to accommodate seismically induced deformations. Therefore, the design scope of codes from countries that have experienced destructive earthquakes and an important number of causalities (e.g., the United States and Japan) has shifted to understand the behavior of earthquake-resistant structures [55].

In Colombia, the first earthquake-resistant building code was introduced in 1984 after the 1983 Mw 5.5 Popayan earthquake [56], which has been one of the most important earthquakes that affected a region of the country resulting in economic losses representing 0.98% of the Gross Domestic Product [57]. Later, a new building regulation was issued in 1998 after the Quindío earthquake, where structural irregularities in stiffness and mass showed to be critical. Additionally,

in such code was introduced the division of the country into three seismic hazard zones (Low, Intermediate, and High) [58]. The latest update of the Colombian Code for Earthquake-resistant Construction, NSR-10 [59], was published in 2010 where a seismic hazard map was reported which was the result of analyzing 28,000 events that included 25 Mw 7.0 and Mw 8.0 quakes considering characteristics such as depth, magnitude, and nature [60]. As claimed in the NSR-10 code, the structures designed must exhibit suitable strength and stiffness when subjected to code-design loads, have adequate stiffness to limit deformability to service loads [59], and guarantee life protection. Moreover, buildings that are designed following standard procedures for the same hazard level and have the same structural system are expected to exhibit comparable seismic risk and performance [61].

Modern earthquake-resistant codes allow ordinary buildings to experience a certain level of structural damage when subjected to design earthquake loads if the inelastic deformations do not jeopardize their safety [62]. Current design practices are based on linear elastic analysis which entails high uncertainty [63], as building performance is not linear when subjected to large earthquakes. The Colombian design procedure uses the conventional force-based displacement-check approach [64] and consists of several phases: first, a preliminary dimension for the structural elements; second, calculation of the elastic design spectrum that corresponds to an earthquake with a return period of 475 years, considering the location of the building. Third, spectral acceleration value (Sa) is selected depending on the fundamental period of the building with gross sections. Fourth, the Sa is used to verify whether the building structural elements are capable to fulfill the drift limit requirement. Once the drift limit requirement is satisfied, the building is designed with the Sa reduced by an energy dissipation capacity factor (R), which value depends on the energy dissipation capacity of the structure.

The core premise behind reducing the spectral acceleration value during the design phase is founded on the expectation that the building's ductility and overstrength will enable it to endure more substantial seismic forces compared to the levels assumed when linear behavior is exceeded. However, the earthquake-resistant codes do not provide an explicit evaluation guideline for the seismic performance of the building beyond the elastic range.

Despite the reliance on code regulations for the earthquake-resistant design of buildings, the seismic performance of the resulting structures in terms of safety level is not explicitly evaluated during the process. Instead, building codes define an overall expected performance in terms of predefined levels such as life safety and collapse prevention. In particular, the NSR-10 code indicates that "a building designed following the standard requirements must be able to withstand low intensity shaking without damage, moderate shaking without structural damage, but possibly with some damage to non-structural elements, and strong shaking with damage to structural and non-structural elements but without collapse" [59]. Nonetheless, it fails in stating explicitly the probability of occurrence of each of those scenarios, and the safety boundaries are not controlled nor quantified as other state-of-art codes (e.g., Eurocode8 [65] and Italian code [66]).

The aforementioned results in a lack of an explicit estimation of the safety level of code-designed buildings that has been acknowledged by researchers who have conducted studies to establish the safety level among structures designed per earthquake-resistant codes. For instance, some studies [67]–[70], used non-linear analyses to assess the seismic behavior of mid-rise reinforced concrete (RC) and steel buildings located in specific seismic hazard regions. In other studies such as [71]–[73], the main goal was to estimate the seismic safety level of existing structures, pointing out the need for more precise control of the seismic performance of the buildings beyond the design code-compliant requirements. One of the key documented studies that

has been developing in Italy is known as the research project Rischio Implicito di strutture progettate secondo le Norme Tecniche per le Costruzioni (RINTC), which is the result of the cooperation between the Network of University Laboratories of Earthquake Engineering and the European Center of Research and Education in Earthquake Engineering [72]. The main goal of such project is to define the seismic risk to which structures are exposed and has been developed by means of analyzing a series of building designs including different structural systems at different hazard levels. This research led to realize that design based on similar hazards does not necessarily entails the same level of risk for the structures. It also helped to reveal that the thresholds stated in the Italian design code are not very conservative when the building is located close to the site of the earthquake epicenter.

Following the same research line, Macedo and Castro [73] assessed the collapse safety margins in steel moment resisting frames designed following the Eurocode 8 (EC8). They evaluated such condition for the maximum considered earthquake level following the methodology proposed by FEMA P695 [74]. The results indicate that the collapse probability of steel frames complies the EC8 no-collapse requirement. Finally, in the RINTC framework, Suzuki and Iervolino [75] conducted a multiple-stripe analysis to evaluate the seismic fragility of structures using the equivalent single degree of freedom (ESDOF) approach. The outcomes of such research showed that the performance results of buildings designed for high-hazard sites are consistent with the calculated in the RINTC.

Although research on the topic has been conducted in different countries, there are no reports in Colombia aimed at stablishing the safety level of buildings designed under similar seismic hazard. Hence, the main goal of this study is to investigate the impact of the design criteria on the

safety level of a benchmark code-compliant RC frame buildings, designed for intermediate seismic hazard conditions according to the NSR-10.

To do so, five cities in the country were selected: Bogotá, Sincelejo, Medellín, Tunja, and Ibagué. Afterward, a five-story RC moment resisting frame building was designed using ETABS software [76] considering the seismic hazard level of each city. Then, the designs were assessed through non-linear static and dynamic analyses to obtain capacity and fragility curves for four damage limits defined in terms of inter-story drift. For this purpose, a pushover analysis, and an incremental dynamic analysis (IDA) [77] were conducted using the Open System for Earthquake Engineering Simulation software (OpenSees) [49]. Measures such as overstrength and probabilities of exceedance of damage are considered in the performance evaluation of this study, mainly at the design base earthquake (DBE) and maximum considered earthquake (MCE) levels.

2.2   Methods

2.2.1   Description of case of study

Figure 2.1 shows the location of the five Colombian cities chosen in the study. The first city is Bogotá, the capital city of Colombia, where approximately 8 million people live [78] and is in the center of the country. Medellín is the second most important city of Colombia with more than 2 million inhabitants and represents an important link in the Antioquia supply chain, which accounts for the second largest contributor to the country's GDP [79]. The third city is Ibagué, a city located 209 km from Bogotá and has a population of more than 500,000 people. Then is Tunja, the main city of the Boyacá state which is in the central east region of the country and has a population of approximately 200,000 million inhabitants. Sincelejo is a city on the north coast of Colombia where more than 300,000 million people live, and it is among the 10 capital cities with

lower income in the country [80]. Overall, these five cities account for 11.5 million people, which represents 22% of the country's population. According to the Administrative National Department of Statistics (DANE is the acronym in Spanish), RC moment resisting frames represent 67% of the residential buildings constructed from 2020 to 2022 in the cities studied [81].
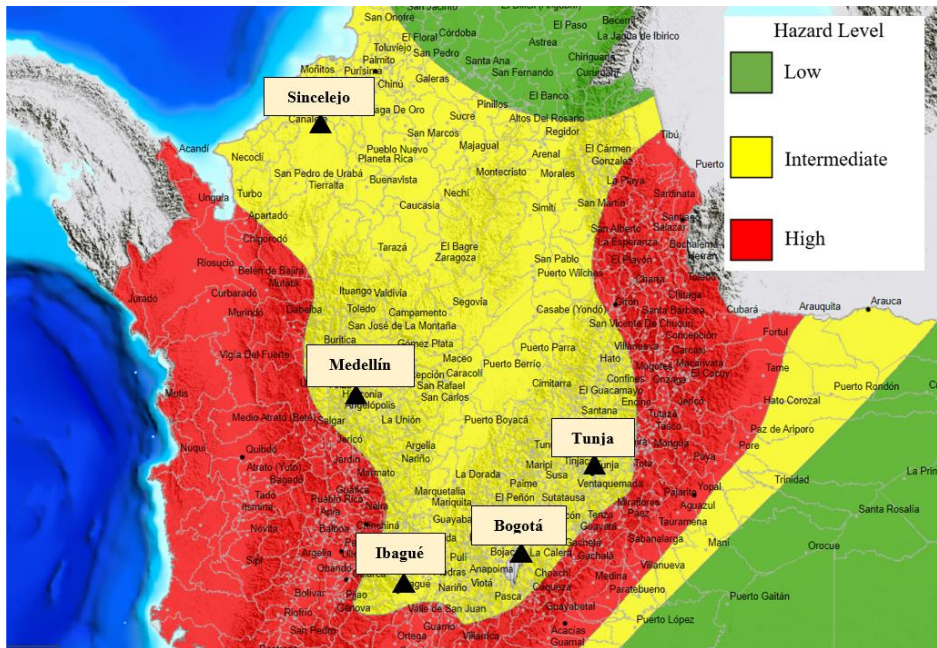
Figure 2.1 Location of cities in Colombia chosen in the study. Source: [82]

A 5-story RC residential MRF building was selected to be designed for each one of the cities and consists of four-bays with an inter-story height of 3 m. The building follows the typical plan layout shown in Figure 2.2(a). Each building was designed according to NSR-10 code, which holds several similarities to the ACI 318-08 [83] for designing RC frames. Following NSR-10, the dead load of non-structural elements and the live load are 2.8 kN/m^2 and 1.8 kN/m^2, respectively, which were applied over the slabs. The preliminary size of the structural elements was calculated through a rapid assessment with approximate methods based on the estimation of the axial load over the columns and the length of the beams.

The building was designed for a D-type soil (Vs values between 180 m/s and 360 m/s), which translates into spectral design acceleration (Sa) values of 0.56 g for Bogotá and Medellín, 0.70g for Ibagué and Tunja, and 0.40 g for Sincelejo. A 3D model (Figure 2b) was developed using ETABS software [76]. The concrete compressive strength (f'_c) chosen for the buildings was 28 MPa, which is a typical concrete strength for this type of buildings in Colombia. For the steel reinforcement, a minimum yield strength (F_y) of 420 MPa and an ultimate tensile strength of 630 MPa were used in accordance with the minimum values required by ASTM A706 [84]. Solid slabs of 12 cm thickness were used and modeled using shell-thin elements. Rigid diaphragms were assumed at each story level. The buildings were analyzed using the modal spectral method checked by the equivalent lateral force method (ELF).

Concerning the verification of compliance with the design drift requirements prescribed by the Colombian code, the final dimensions of the structural elements were selected in such a way that the inter-story drift calculated using gross sections did not exceed 1%. This threshold is stricter than the limits of other codes such as the ASCE 7, but research has shown that this fact does not mean higher safety levels [83]. In addition, these drift limit values are more related to serviceability than collapse prevention, as the main goal is to prevent non-structural damage which is considered a critical issue due to the country's economic limitations [64].
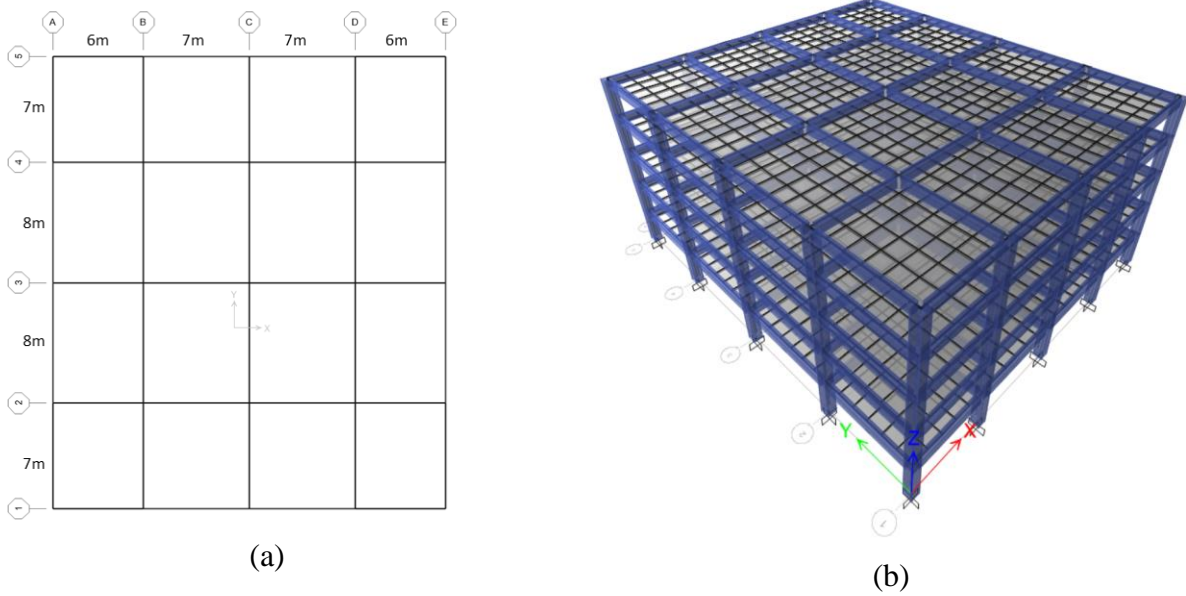
Figure 2.2. Archetype of a five-story four-bay RC frame building; (a) typical plan view and (b) 3-D model

2.2.2 Nonlinear Models

Two-dimensional models were constructed using OpenSees software [49] to evaluate the seismic performance of the buildings. The 2D representation corresponds to frame number 3 shown in Figure 2.2a since it accounts for one of the frames with the largest tributary area. The models were analyzed by means of non-linear static (Pushover) and dynamic analysis (IDA) using a distributed plasticity approach considering fixed base. ForceBeamColumn [85] elements with fibers were used to model the beams and the columns. A rigid diaphragm was considered by applying an EqualDOF constraint to the model.

In terms of material properties, the confined and unconfined concrete were modeled as Concrete01 uniaxial material. For the unconfined concrete, a maximum compressive strength of 28 MPa and a peak compressive strain of 0.0023 were considered. For the confined concrete, the Mander model [86] was used and a peak compressive strength of 36.4 MPa was calculated with a

peak strain of 0.0030. For both models, the residual concrete strength was assumed to be 20% of its peak value.

Furthermore, since strain localization issues has been encountered in numerical models that use force-based elements, a regularization technique based on the constant fracture energy was applied [87]. The fracture energy constant was set to the value of the peak compression stress for unconfined concrete and twice the peak compression stress value for confined concrete. The ultimate strain for both concretes were set to the value obtained with the regularization. The reinforcement steel was modeled using the Hysteretic material available in Opensees and the properties considered correspond to the reinforcement steel commercialized in Colombia, which was studied by Carrillo *et al*. [88]. The Hysteretic material model can be modified to capture steel rupture and buckling by leveraging the "MinMax" material model in OpenSees [89]. Therefore, the MinMax material was used together with the Hysteretic to specify an upper and lower limit of the reinforcement strain. For this research, the thresholds were set to -0.008 to account for the bar buckling that follows the spalling of the concrete, and 0.05 to represent the low cycle fatigue of the steel [90]. Once the strain exceeds the predefined limits, the material ceases to function, representing the rupture. The backbone curve for the steel and one example for the concretes are presented in Figure 2.3a and b.
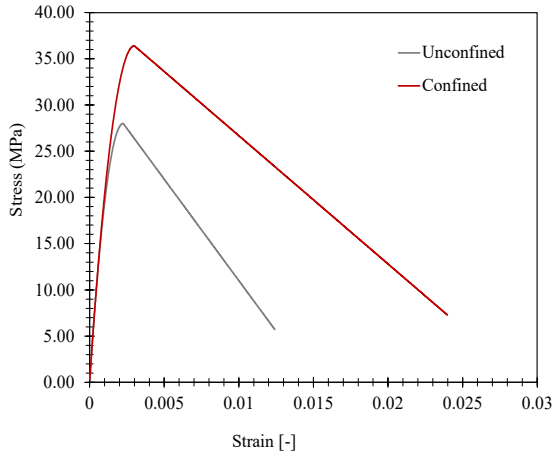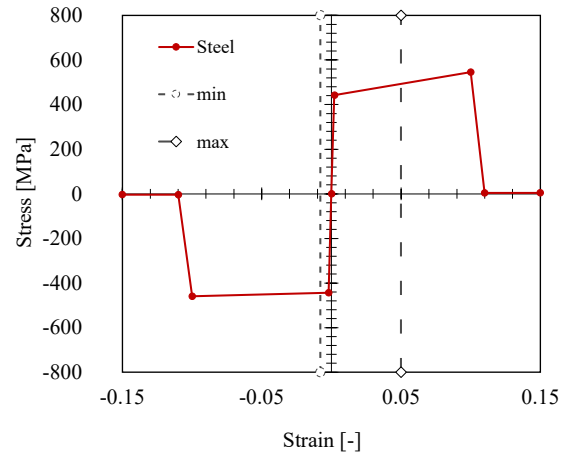
Figure 2.3. Materials backbone curves. (a) Backbone curve of unconfined concrete of the columns and (b) backbone curve of the reinforcement steel

2.2.3 Pushover Analysis

Static pushover analysis is a method to evaluate the actual strength of the building and has been a useful and effective tool for performance-based design [91]. An inverted triangular load pattern proportional to the product of the masses times their heights was applied for the pushover analysis. This type of pattern is widely used in literature and is considered appropriate for mid-rise buildings [92] such as the one in this study. The analysis was conducted using a displacement control integration scheme with 0.001 mm steps until a target displacement of 4% of the roof drift was reached. A plain approach was applied to handle the constraints of the model. Additionally, the Reverse CuthillMcKee (RCM) numberer object was selected for numbering the degrees of freedom of the structure. The Newton solver method was chosen with an EnergyIncrement convergence test with a tolerance of 1×10^{-8}.

2.2.4 Incremental Dynamic Analysis

Incremental Dynamic Analysis (IDA) is a widely used method for estimating structural behavior under seismic loading by subjecting the structure to a suite of ground motion records each of one scaled to different intensity levels [77]. For this analysis, the set of 44 ground motions proposed by FEMA P-695 was chosen [74] since approximately 80% of the Colombian territory

is prone to be affected by crustal earthquakes [51]. It was deemed appropriate to use the suite for the analyses.

The models used the Rayleigh damping approach proportional to the mass and current stiffness matrix, with damping of 3% of the first and third modes of vibration as suggested by Deierlein *et al*. [93]. The seismic masses were lumped at the nodes of the model and were calculated considering its tributary area.

Based on the information available in the records, the acceleration spectrum for each earthquake was generated and subsequently scaled to the design level of the building spectral acceleration for each city. Then, each ground motion was affected with the following scale factors: 0.25, 0.5, 1.0, 1.5, 2.0, 3.0 and 4.5 times the design acceleration, where 1.0 represents the design base earthquake (DBE) and 1.5 the maximum considered earthquake (MCE). The time increment used for the analysis corresponds to the time increment of each ground motion.

The inter-story drift ratio (IDR) was selected as the engineering demand parameter (EDP) to assess the building performance in the fragility analysis. The exceedance of four values of IDR was measured; i.e, 0.33%, 0.58%, 1.56% and 4%. Finally, the results are adjusted to a lognormal cumulative distribution using the following expression:

$$P(C|IM = x) = \Phi\left(\frac{\ln(x/\theta)}{\beta}\right) \qquad \text{Equation 2.1}$$

Where $P(C|IM = x)$ describes the probability that the structure presents collapse given a certain intensity measure (IM). Φ is the standard normal cumulative distribution function; θ is the median of the fragility function and β is the standard deviation of ln IM [94].

2.3   Results and Discussion

2.3.1   Earthquake resistant-code compliant designs

Table 2.1 and **¡Error! No se encuentra el origen de la referencia.** summarize the design results for the cities; the diameters of the steel bars are expressed in octaves of inch. The columns dimensions vary from 0.55 m in the case of Sincelejo to 0.70 m for Tunja; in the case of the beams the values ranged between 0.40 m and 0.45 m for the base, and 0.55 m and 0.65 m for the height. The structural elements were not defined with the same geometrical properties for the cities that share the same value of design spectral acceleration because the main idea was to characterize the variety of design criteria used by practicing engineers. The building with the smallest structural elements is the one designed for Sincelejo since its design spectral acceleration (0.40 g) is the smallest value, which translates into lower seismic demand than the other cities considered. On the other hand, the stiffest design resulted for Tunja since its Sa value is the largest. The table also shows the longitudinal and transverse rebar for both columns and beams, which were considered in the nonlinear models. In the **¡Error! No se encuentra el origen de la referencia.** the design r einforcement ratio for the beams and columns is presented. The reinforcement ratio was set such that the strong coulmn – weak beam is assured.

Table 2.1. Structural elements dimensions and steel rebar for columns.

City	Sa [g]	b [m]	h [m]	Long. Rebar	Transverse Rebar
Bogotá	0.56	0.60	0.60	22 # 6	#3 @ 14 cm
Sincelejo	0.40	0.55	0.55	18 # 6	#3 @ 10 cm
Tunja	0.70	0.70	0.70	22 # 7	#3 @ 16 cm
Medellín	0.56	0.65	0.65	22 # 7	#3 @ 15 cm
Ibagué	0.70	0.65	0.65	22 # 6	#3 @ 15 cm

Table 2.2 Structural elements dimensions and steel rebar for beams.

City	Sa [g]	b [m]	H [m]	Long. Rebar Top	Long. Rebar Bottom	Transverse Rebar
Bogotá	0.56	0.40	0.60	5 # 7	5 # 5	#3 @ 14 cm
Sincelejo	0.40	0.45	0.55	6 # 7	5 # 5	#3 @ 10 cm
Tunja	0.70	0.40	0.60	6 # 7	5 # 6	#3 @ 14 cm
Medellín	0.56	0.40	0.55	6 # 7	4 # 6	#3 @ 13 cm
Ibagué	0.70	0.45	0.65	6 # 7	6 # 5	#3 @ 15 cm

Table 2.3 Designs reinforcement ratio

City	Design ID	ρ [%] Columns	ρ [%] Beams
Tunja	0.70-1	1.7	1.5
Ibagué	0.70-2	1.5	1.2
Bogotá	0.56-1	1.7	1.2
Medellín	0.56-2	2.0	1.6
Sincelejo	0.40	1.7	1.3

Table 2.4 shows the maximum inter-story drift for each building. Those values are remarkably close to the threshold prescribed by the NSR-10 Colombian code (1%) because, in practice, the reduction of the structural elements size criteria is the mean used by designers in order to get an optimal design that balances the total cost of the construction and the requirements prescribed by the code. The structural period is also shown for the buildings modeled elastic and non-linearly. The elastic approach exhibits larger periods of vibration for the buildings, meaning they are less stiff when modeled linearly. The non-linear model exhibits lower period meaning an increment on the buildings stiffness that is caused by its material configuration where the presence of the steel reinforcement is considered. Moreover, the structural periods vary for both elastic and

inelastic models in buildings designed for the same spectral acceleration due to the design criteria, reflected in the conception of different sizes for structural elements and steel rebar.

Table 2.4. Maximum inter-story drift ratio and natural structural periods

City	Max. Drift.		Period [s]	
	x	y	Elastic	Non – linear
Bogotá	0.86%	0.94%	0.69	0.67
Sincelejo	0.90%	0.98%	0.76	0.74
Tunja	0.88%	0.97%	0.63	0.58
Medellín	0.89%	0.97%	0.70	0.64
Ibagué	0.82%	0.90%	0.60	0.56

2.3.2 Pushover Analysis

In this section, the results obtained from the pushover analysis are shown in terms of base shear and overstrength, the latter is the result of dividing the base shear obtained by the design shear of the building (Y-axis), and roof displacement, and roof drift, which represents the ratio between roof displacement and the total height of the building (X-axis).
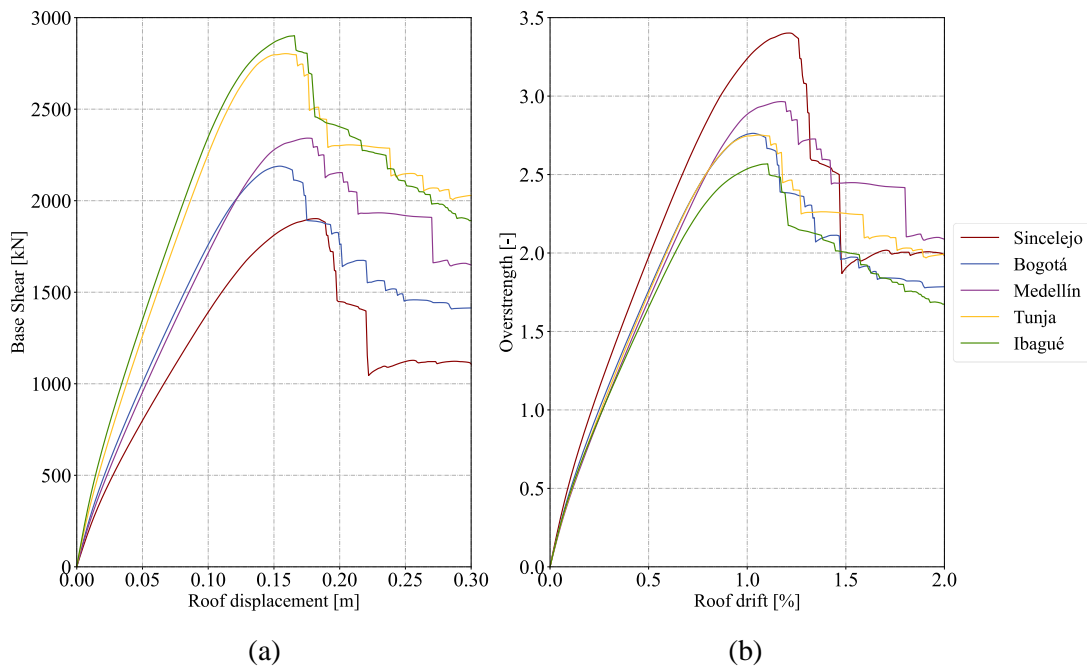

(a)　　　　　　　　　　　(b)

Figure 2.4. (a) Base shear vs roof displacement and (b) overstrength vs. roof drift

23

Figure 2.4 shows the capacity curves of the five buildings. The capacity curves of the buildings that share the same Sa differ, this can be attributed to the variation in the geometry and steel rebar of the columns. From now on, Tunja and Ibagué buildings will be reffered as 0.70-1 and 0.70-2 designs, respectively; Bogotá and Medellín will be 0.56-1 and 0.56-2, and Sincelejo as 0.40. The building's overstrength appears to rise with a higher reinforcement ratio when designed for the same Sa value. For instance, structures with ratios of 0.56-2 and 0.70-1 demonstrate increased overstrength compared to their counterparts with lower amounts of reinforcement steel.

As the slope of the curve in the elastic range can be related to the stiffness of the structure, it can be seen that the 0.70 buildings designed are stiffer than those designed for lower values, as the slope in the elastic range tends to be steeper. Figure 2.4b shows a comparison of the overstrength for each building. The overstrength value of the building designed for Sincelejo is over the minimum required by the NSR-10 (2.5), such value means that the building can withstand base shear values that exceeds three times the design shear. On the other hand, the overstrength obtained for the other buildings accomplish with the minimum value. This indicates that as expected by the design considerations, the buildings are able to withstand 2.5 times the base shear beyond their elastic state.

Another highlight of the buildings behavior is that the point of first capacity loss (the first fall in the capacity curve) differs from 0.56-1 to 0.56-2 by 10 cm of roof displacement. Additionally, 0.56-2 exhibits better ductlity than 0.56-1. On the other hand, the overstrength values calculated for the 0.70 buildings were 2.8 and 2.6 (for 0.70-1 and 0.70-2, respectively), this means that for Sa values of 0.70 a better performance in terms of overstrength can be pursued following the 0.70-1 desing. which is bellow the minimum required by the colombian earthquake resistant code. In terms of capacity loss and cutility, both buildings describe a very similar behavior.

The performance of the buildings is further examined by means of the drift profiles shown in Figure 2.5. The results are presented for different roof drifts: 0.9%, 1% where the first pushover, and 1.2%.
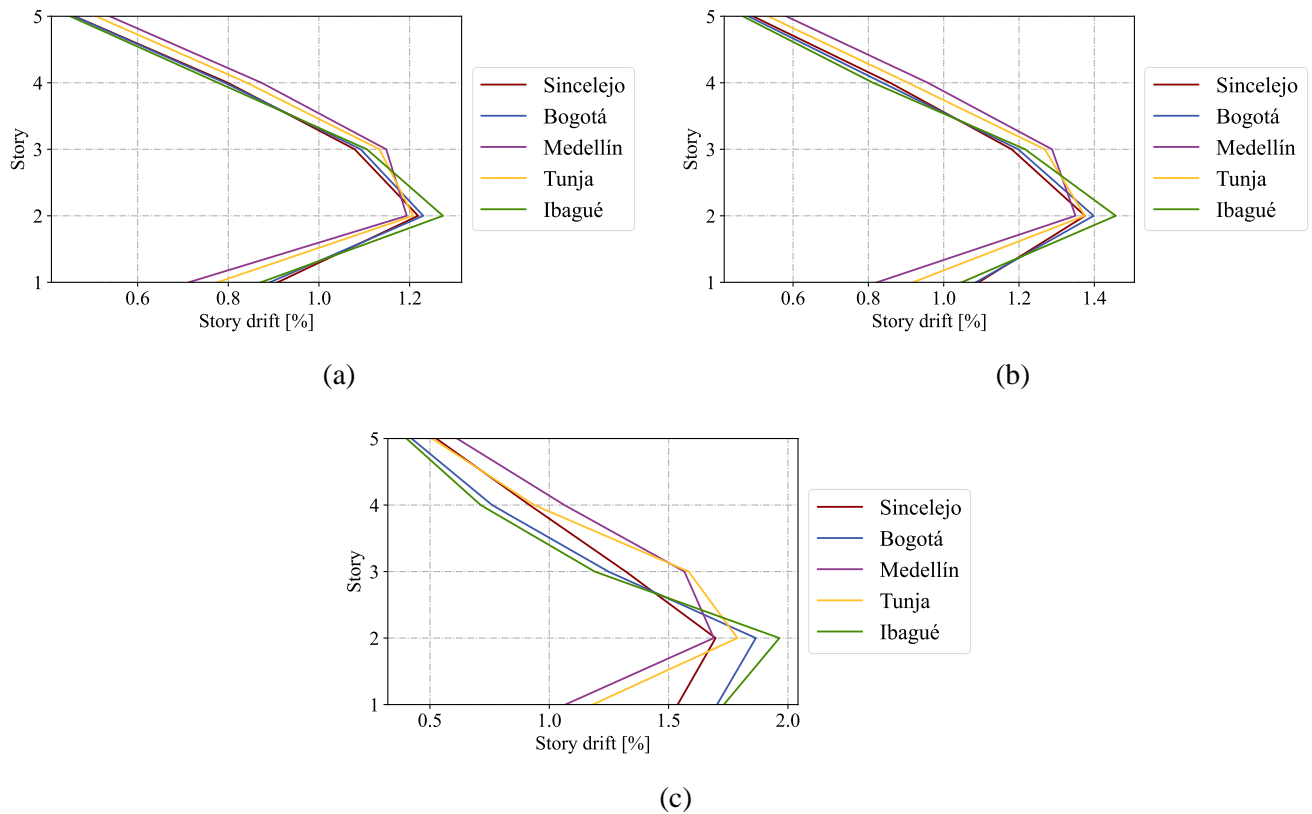
Figure 2.5. Pushover story drift distribution evaluated at different limits; (a) Roof drift of 0.9%, (b) roof drift of 1%, and (c) roof drift of 1.2%

In general, there is a clear tendency for damage accumulation on the second floor. Such behavior implies that as damage occurs, it concentrates on the lower stories. Moreover, the drift profiles show that the 0.70-2 building (Ibagué) has greater story drift on the second floor compared to the rest. Additionally, for a roof drift of 0.9%, the story drift obtained for all the buildings exceeds the limit of 1% of the NSR-10 Code. In the 1.2% of roof drift (Figure 2.5c), the 0.56-, 0.70-2 and 0.40 buildings (Bogotá and Sincelejo) show weak floor mechanism, which can be an explaination of the sudden falls presented in the capacity curves. On the other hand, the performance of the 0.70-1 and 0.56-2 buildings is quite different since the drift profile obtained suggests that the damage spreads in a larger portion of the structure.

Based on the overall results of the pushover analysis, the seismic performance of the buildings designed for the same seismic intensity level is prone to be affected by two main aspects: the structural elements geometry and the reinforcement. Such results led to state that design criteria

25

exert an important influence in the safety level of structures designed following earthquake-resistant code guidelines.

2.3.3   Incremental Dynamic Analysis

The structural performance of the buildings was also assessed by conducting an Incremental Dynamic Analysis, which involves scaling a suite of ground motion records to force the structure to perform beyond the elasticity state to a final global dynamic instability [95]. The results obtained for such analysis are presented in this section. Figure 2.6 presents the IDA curves for each design. The median curve distribution (presented in black) for the designs supports the pushover results since the 0.56-2 and 0.70-1 exhibit lower values of inter-story drifts compared to their counterparts. Another highlight from the IDA curves is that at the DBE level (Scale Factor = 1.0) the maximum inter-story drift values are over 1%, which indicates that the drift restriction prescribed in the NSR-10 is not fully complied.
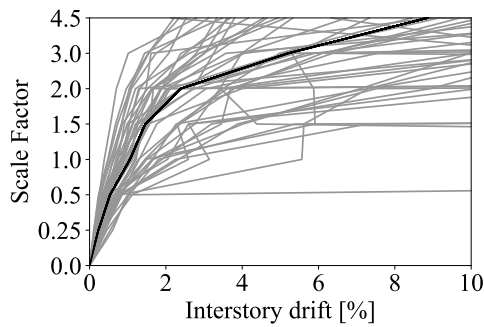
(a)
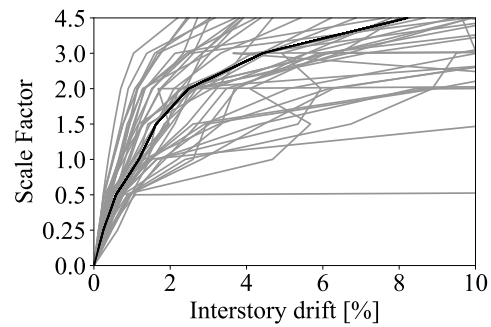
(b)
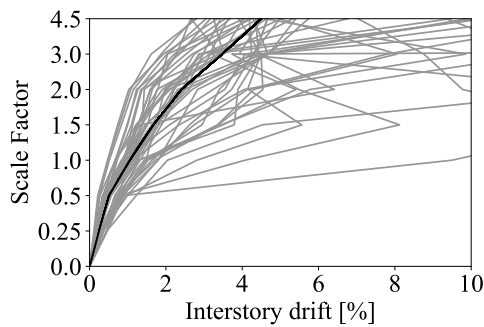
(c)
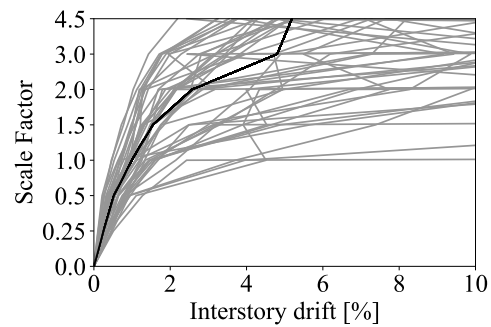
(d)
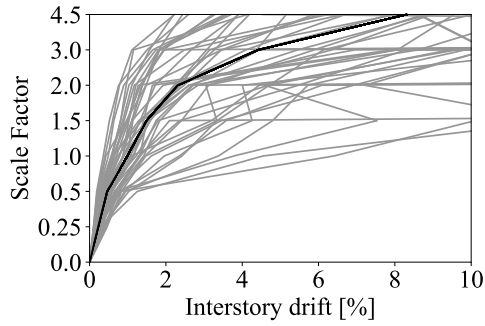
(e)

Figure 2.6 IDA curves. (a) Bogotá; (b) Medellín; (c) Tunja; (d) Ibagué, (e) Sincelejo.

Figure 2.7 and Figure 2.8 show the fragility curves for buildings of different cities designed for 0.56 and 0.70 Sa values. The results show a significant difference in the 1% limit, at which Bogotá and Ibagué buildings perform more fragile than Medellín and Tunja. Alternatively, the variations in building fragility across the remaining limits are less than 1.0%. In fact, the fragility curves for these limits exhibit striking similarity.
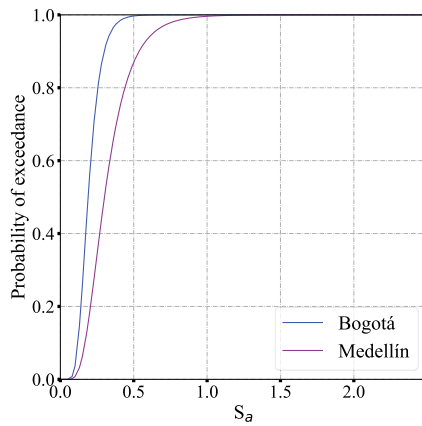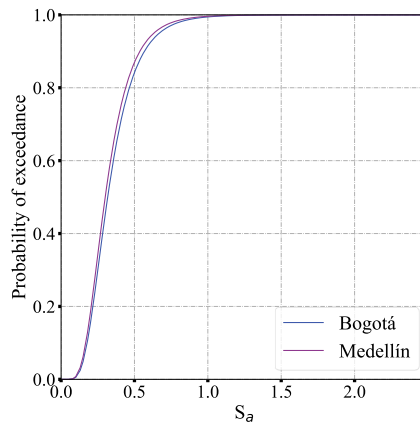
(a)   (b)
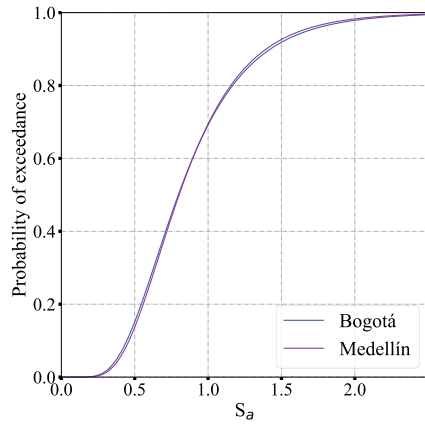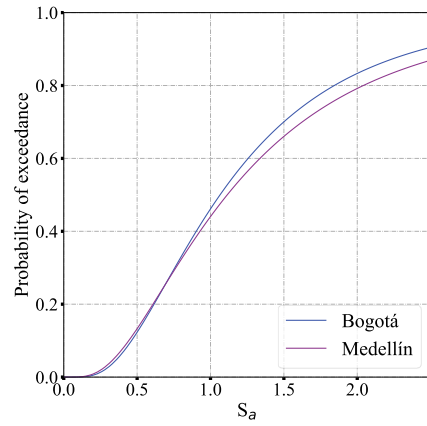
(c)   (d)

Figure 2.7. Fragility curves for Bogotá and Medellín buildings; (a) for EDP of 0.33%, (b) for EDP of 0.58%, (c) for EDP of 1.56%, and (d) for EDP of 4%
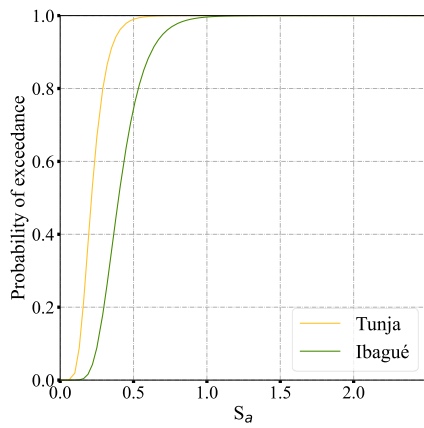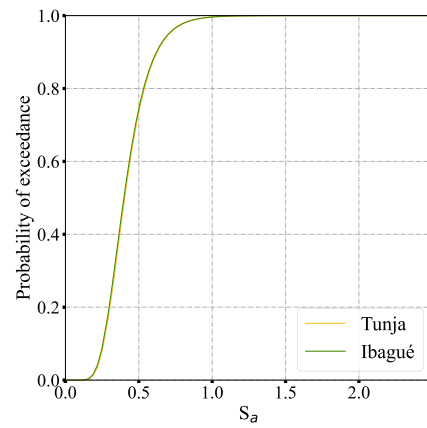
(a)   (b)
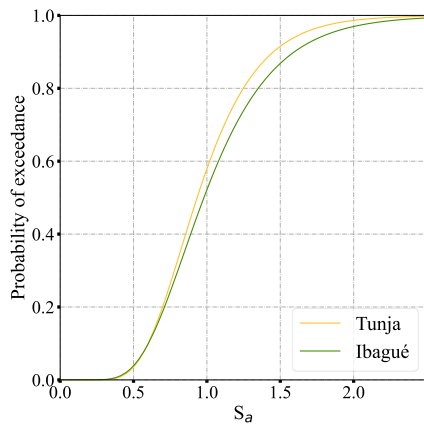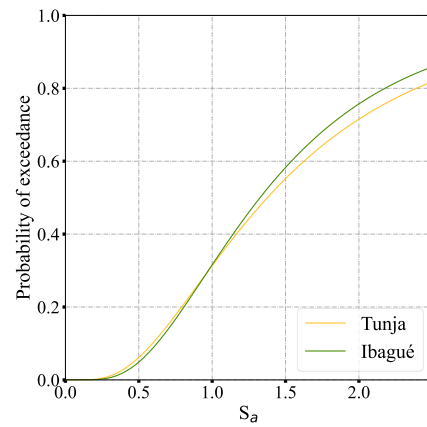
(c)   (d)

Figure 2.8. Fragility curves for Tunja and Ibagué buildings; (a) for EDP of 0.33%, (b) for EDP of 0.58%, (c) for EDP of 1.56%, and (d) for EDP of 4%

Figure 2.9 shows the fragility results with the intensity measure normalized by the design acceleration of each building. The main idea of such normalization is to ensure that the performance results of buildings designed for different cities are comparable; this is possible since the scale factors used in the dynamic analysis for every city are the same. For the 0.58% limit, evaluating the DBE condition, the building designed for Sincelejo has less than 50% probability of exceedance, while the other buildings have more than 50%. On the other hand, when an inter-story drift of 1.58% is considered as EDP (Figure 2.9b), the probability reported is less than 20% for all buildings at DBE level. However, at the MCE level (Sa/SaDesign = 1.5), the probability values of the building designed for Sincelejo is lower than the values obtained for other buildings. In addition, at that level, the designs for the other cities reach the same probability.
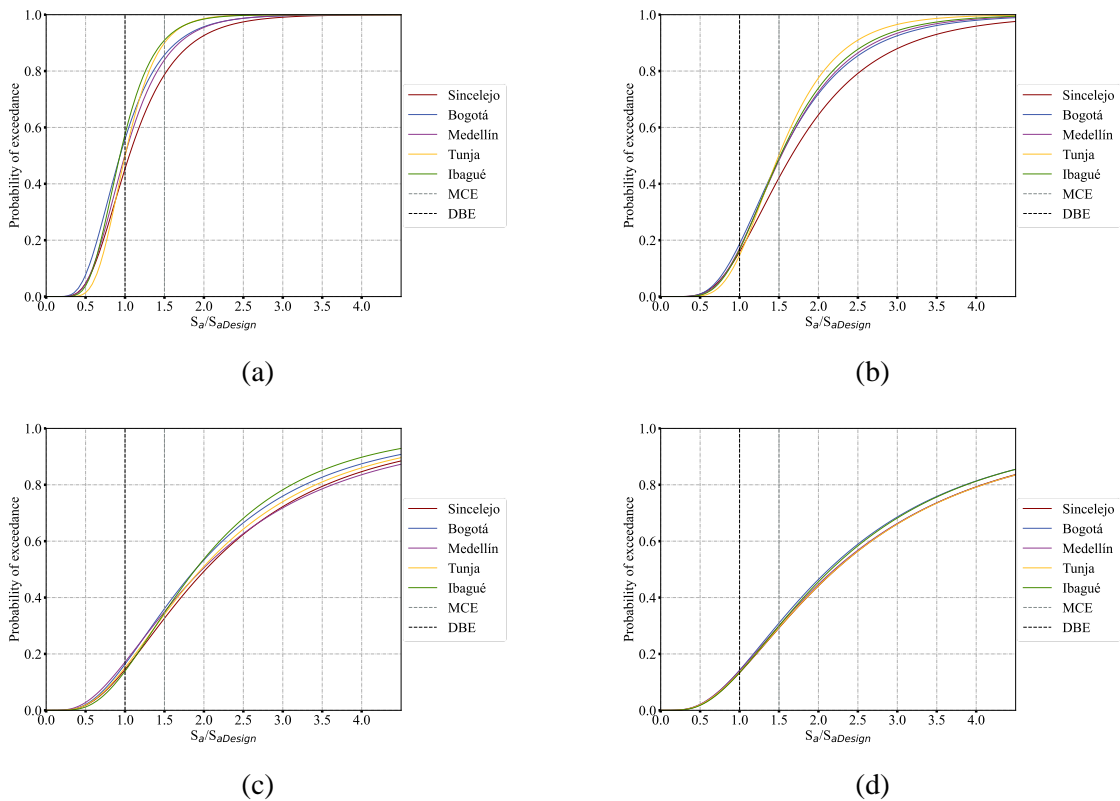
Figure 2.9. Fragility curves normalized by design Sa; (a) for EDP of 0.33%, (b) for EDP of 0.56%, (c) for EDP of 1.58%, and (d) for EDP of 4%

The fragility curves obtained for an inter-story drift limit of 1.58% are shown in Figure 2.9c. The buildings that share the same Sa show very close exceedance probabilities at both DBE and MCE levels. In addition, at this damage threshold, the exceedance probability calculated for the building of Sincelejo is lower at the MCE level, however such difference is not very large. Figure 2.9d shows that the fragility values for the exceedance of 4% of inter-story drift are very close for all the buildings at both DBE and MCE.

The fragility results are further analyzed by obtaining the β and θ parameters, which represents the dispersion obtained from curve fitting and the ground motion intensity that has 50% of occurrence of the limit state, respectively. Table 2.5 presents these values for the five buildings along with θ normalized by the design acceleration of each building.

The findings show that for each limit state considered in this study, the intensity value at which the 50% of the exceedance probability is reached differs when comparing the five buildings, especially considering the Sincelejo design. However, such values for the buildings designed for the same value of Sa are similar ranging between 2% and 8%. Such values indicate that the buildings reach 50% of exceedance probability at very similar intensity measures.

Table 2.5. Statistical parameters for the lognormal fitting of the fragility curves.

δ	City	θ	β	θ/Sa_Design
	Bogotá	0.527	0.441	0.937
	Medellín	0.561	0.411	0.997
0.33%	Ibagué	0.701	0.316	1.001
	Tunja	0.655	0.353	0.935
	Sincelejo	0.421	0.443	1.053
	Bogotá	0.856	0.471	1.521
	Medellín	0.860	0.447	1.529
0.56%	Ibagué	1.048	0.383	1.496
	Tunja	1.062	0.431	1.517
	Sincelejo	0.663	0.505	1.658
	Bogotá	1.065	0.652	1.893
	Medellín	1.114	0.720	1.980
1.56%	Ibagué	1.376	0.657	1.966
	Tunja	1.326	0.589	1.895
	Sincelejo	0.810	0.666	2.024

δ	City	θ	β	θ/Sa_Design
	Bogotá	1.199	0.707	2.131
	Medellín	1.240	0.733	2.205
4.00%	Ibagué	1.556	0.724	2.223
	Tunja	1.512	0.694	2.160
	Sincelejo	0.889	0.720	2.224

Lastly, the fragility results are similar those reported by [83] who designed and analyzed a low-rise reinforced concrete frame building according to the United States, Ecuador and Colombian standards. The exceedance probabilities for collapse prevention (which was taken as 6% of inter-story drift) are calculated in terms of MCE intensities. At the MCE level, the probability documented in the reference study was around 20% while the archetype studied in this paper presented values of at most 24% (see Figure 2.9). Moreover, at an intensity level of twice the MCE level the probabilities reported are approximately 75% in the cited study, and range between 60% and 70% for the buildings of this study. Based on the results of the dynamic analyses, some aspects can be pointed out: first, buildings designed for the same level of seismic acceleration exhibit comparable fragility when limits greater than 1% are evaluated. At 0.33%, those buildings whose design contemplated larger beams and columns showed lower probabilities of damage, this behavior can be attributed to their stiffness.

2.4 Conclusions

This research presents the results of the seismic performance of a five-story residential RC moment resisting frame building designed for five Colombian cities located in intermediate seismic hazard zones according to the prescriptions of the Colombian Earthquake-resistant code (NSR-10). To evaluate the performance, the buildings were analyzed using Pushover and IDA in Opensees. The results of the analysis provide information about the lateral capacity of the buildings and the calculation of fragility curves for four damage limits. The findings of this study support the following conclusions:

- The buildings designed following the prescriptions of NSR-10 fulfill the requirements of maximum inter-story drift and the pushover results show that the five designs met the minimum overstrength value suggested per NSR-10 for RC MRF buildings. From the

pushover analysis, it was noted that the buildings with larger sections and larger steel reinforcement ratios were more ductile and exhibit more overstrength compared to their counterparts.

- The results of the IDAs show that the seismic performance of buildings designed for the same spectral acceleration may vary mainly when low limits of inter-story drifts are evaluated and the buildings with smaller dimensions of structural elements and steel rebar behave more fragile. However, when the spectral acceleration analysis is normalized by the design acceleration, the difference decreases.

Overall, the findings of this study demonstrate that the design criteria followed to define the structural elements and reinforcement in buildings exerts an influence in their seismic performance. Future work in this topic can be pursued in different directions. First, develop a similar study accounting for the local effects. This could be done considering the records available for the country or generating synthetic accelerograms that meet the country seismic characteristics and accommodate to the local effects. Second, assess different types of structural systems, heights, or irregular RC frame buildings to expand the variety of designs that can be conceived by practicing engineers.

3 Chapter III: Fragility curves of mid-rise RC framed, and thin-walled buildings, considering soil-structure interaction, located in Bogotá, Colombia

3.1 Introduction

Estimating the seismic performance of a structure has become an issue of great importance in the past decades as a response to seismic events that have severely affected many countries such as Turkey, Ecuador, Guatemala, Haiti, Iran, India, Mexico, Japan, and Colombia, resulting in over a million deaths [96]. In fact, state-of-the art codes establish certain performance levels that the structure must exhibit after an earthquake event [97]. However, in many cases, the customary design assumes that the structure is fixed on its base, which means that the underlying soil is a rock or exhibits high stiffness. Such assumption is deemed as inappropriate for granular and soft soils where additional phenomena can be present [98]. Indeed, experience with past earthquakes (i.e., Mexico City, 1985 (Mw 8.1)) has revealed that the structural damage depends on the behavior of the soil beneath [4] [5]. The linking condition among the soil, the foundation, and the structure is known as Soil-Structure Interaction (SSI) and consists of the evaluation of the collective response of the three systems to a specific ground motion [99].

Early SSI calculations involved complex arithmetic expressions to relate wave propagation, which made the interaction difficult to comprehend [9]. Over the years and along with the advancements in computer science, such condition was overcome leading to the generation of more efficient mathematical models that could be analyzed faster. Such models allow to evaluate the two main components in the SSI: *kinematical* and *inertial*. The former arises from the presence of the foundation elements in the soil, which modifies the input motion that the structure

undergoes, and the latter refers to the effect that the structure inertia has on the behavior of the foundation. The inertial interaction results into two main effects: structural period lengthening and damping modification [22]. There are two broad known techniques to model SSI, the exhaustive technique is called the *direct method* where the structure and the soil are modeled with finite elements that are used to capture the nonlinearities in both soil and structure. The second technique is called *substructure* where the soil and the structure are studied as two separated systems. The result of the study of the soil-pile interaction is later transmitted to the structure by means of springs and dashpots that represent stiffness and damping [99].

The interest in studying the effect of SSI on buildings has raised among researchers over the years and early studies showed that the performance of structures founded on medium to soft soils is remarkably affected when the SSI is considered [35], [100], [101]. More recent works have focused on evaluating SSI influence on structure fragility by varying the foundation soil-type. One of the most studied structural systems are moment resisting frames of which a wide variety of studies are available. For instance, Tapia-Hernández *et al.* [102] studied the SSI in steel frames of 8 and 12 stories buildings founded in soft soils from the Mexico City lakebed via Pushover analysis. The authors findings led to state that SSI should not be neglected specially for the piled-founded case, since the lateral stiffness of the structure showed to be strongly dependent of the group effect on piles. Another work was developed by Oz *et al.* [42] who by means of a time history analysis (THA) studied the SSI effects on the response of 40 existing low and mid-rise RC buildings in Turkey for four conditions: fixed base, stiff, medium, and soft soils. Half of the buildings were designed with the current earthquake-resistant regulations and half were designed with the previous one. The results pointed out that the SSI affected principally the old buildings on weak soil conditions where large values of drifts and collapses were calculated. In the same

line, Forcellini [103] evaluated the seismic fragility of a RC walls and steel columns 20-story building founded on piles considering SSI via 3D finite element modeling and his results showed that ignoring the SSI may lead to underestimate the vulnerability in the entire system (i.e., soil-foundation-superstructure). Likewise, Anvarsamarin *et al.* [41] reported that by considering the SSI in the fragility analysis of RC moment resisting buildings of 6, 12 and 18 stories modeled in 3D, the median of intensity measure of the fragility curves reduces by 4.94%, 22.26%, and 23.03% in each case, which means that the structure is more fragile as it reaches certain damage level at lower intensities.

Another structural system that has recently attracted the attention of researchers is the thin wall system also known as industrialized system that has become popular in residential construction specially for low and mid-rise buildings in Latin-American countries with high seismicity (i.e., Colombia, Peru, Mexico, and Chile [104]. The assessment of the structural fragility of buildings with RC thin walls has been reported by some authors [31], [105]–[108] who highlight the need of limiting the use of RC thin walls in seismic prone areas specially when the reinforcement consist of welded-wire-mesh (WWM), since the failure mode of such buildings is highly influenced by the fracture of the steel. The authors did not come across any studies on RC thin-walled buildings that incorporated SSI. However, there are reports of studies in conventional RC walls, some of them aimed to evaluating the changes that SSI induced in the foundation sizing due to settlements redistribution [109]; other studies aimed to assessing the seismic performance such as the conducted by Carbonari *et al.* [47], [48], evaluated the fragility of a coupled wall-frame system modeled linear and nonlinearly considering SSI for three different soil profiles. The findings support the importance of considering SSI effects on the seismic performance of the building given the significant increase in lateral deformability of the whole structure, leading to

35

earlier damage in the structural and non-structural elements. In the study conducted by Rodríguez *et al.* [110], significant differences were observed in the fragility curves when comparing the fixed base approach to the consideration of SSI. The researchers utilized Incremental Dynamic Analysis (IDA) [95] to calculate fragility curves for a 20-story RC walls Chilean residential building with shallow foundation using the Open System for Earthquake Engineering Simulation (OpenSees). The study revealed changes in the medians of the fragility curves, with slight to moderate damage states increasing 33% and 57%, respectively. Notably, the fixed-base model did not reach the extensive and collapse damage states, in contrast to the results obtained with the SSI model.

As mentioned previously, the influence of soil-structure interaction (SSI) becomes more pronounced in the case of soft soil properties. This effect is particularly evident in cities like Mexico City, situated within the Mexico Valley, where the central area is characterized by deposits of lacustrine soft clay [111]. The phenomenon has been widely studied and reported [21]–[26], [112] specially after finding that the geotechnic and topographic setting of the beneath soil has remarkably influenced the structural behavior of buildings during past earthquakes (i.e., Mw 8.1 in 1985 and Mw 7.1 2017) [113]. A geotechnical counterpart of Mexico City is Bogotá, the capital city of Colombia with a population that represents 15% of the country's population [78]. The city has undergone a rapid urban development specially towards the Sabana lands, which consist of lacustrine soft soils. This type of soils might act as a seismic wave amplification mechanism, so the damage experienced by the buildings founded in such soils can be remarkably higher than the experienced by the buildings founded on more resistant soils [27], as in Mexico City. However, in Bogotá the only study of SSI effect in the seismic performance of a building known to the authors is the Bahamon-Mejía thesis [32], in which a 10-stories RC frame building located in the lacustrine soils of the city was analyzed via Pushover and considering the substructure and the linear behavior

of soil. Therefore, a knowledge gap is identified since there are not reports of studies that consider buildings of different heights or structural systems, nor the nonlinear behavior of the soil.

Considering the Bogotá case, this paper aims to study the effect that SSI exerts in the fragility of two mid-rise RC buildings, one with moment resisting frames structural system and the second with RC thin walls. These structural systems accounts for more than 10% of the buildings stock in Bogotá [104], [114]. The buildings were chosen to be founded in five locations within the lacustrine soils of Bogotá, for which the foundation was designed in accordance with the soil properties following the section H of the Colombian design regulations.

For the structural analysis, two dimensional models were developed using OpenSees [49] for three conditions (i.e., fixed base, flexible base with linear and nonlinear soil characteristics). The soil was modeled using *zerolength* elements with elastic uniaxial materials for the linear case and with *PySimple1*, *TzSimple1* and *QzSimple1* materials for the nonlinear case. The foundation was modeled elastically with gross sections that follow the design for each location, while the superstructures was modeled using two kinds of elements: for the RC frames a distributed plasticity approach with *force-based* elements with fibers was used, while the RC thin walls were modeled using *multiple-vertical-line-element-model* (MVLEM) [115]. The models were analyzed via Pushover and Dynamic analysis to obtain capacity and fragility curves.

3.2   Methodology

3.2.1   Buildings structural characteristics

The chosen frame building follows the plan shown in Figure 3.1a and consists of a four-bay five story RC moment resisting frame with inter-story height of 3 m. The superstructure was designed in accordance with current Colombian earthquake-resistant code provisions for a fixed

base condition for superimposed dead and live loads values of 2.8 kN/m^2 and 1.8 kN/m^2, respectively. The structural elements dimensions were chosen such that the strong column – weak beam relation, of 1.2 was granted and the inter-story drifts did not exceed 1%, since it is a requirement prescribed in the Colombian standard [59]. Table 3.1 summarizes the geometrical and reinforcement characteristics of the superstructure. The second building to analyze corresponds to an existing 6-stories RC thin wall residential building with a concrete strength of 21 MPa. Each wall has 10 cm of thickness and follows the plan layout shown in Figure 3.1b. The inter-story height is 2.45 m, so the total height of the building is 14.7 m. The steel reinforcement consists of a welded-wire-mesh (WWM).
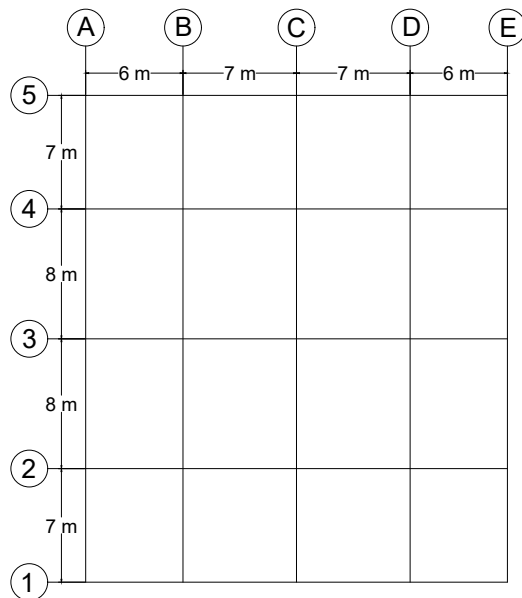
(a)
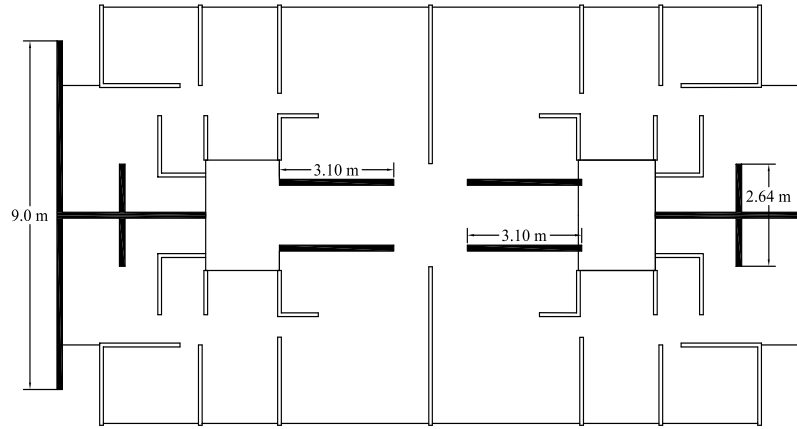
(b)

Figure 3.1 Typical plan view of the buildings studied. (a) RC frame building (b) RC thin wall building

Table 3.1 Beams and columns design

Beams						
b	h	Steel reinf. Ratio		Long. Rebar		Transverse Rebar
[m]	[m]	Top	Bottom	Top	Bottom	
0.4	0.6	0.82%	0.39%	5 # 7	5 # 5	#3 @ 14 cm

Columns				
b	h	Steel reinf. Ratio	Long. Rebar	Transverse Rebar
[m]	[m]			
0.6	0.6	1%	20 # 5	#3 @ 14 cm

The foundation of both buildings was designed for vertical and seismic loads (the latter accounts for the vertical load multiplied by the horizontal peak effective acceleration coefficient of Bogotá, $Av = 0.15$) for five locations in the city (Figure 3.2) where Bore Holes (BH) information

from the exploration is available in the Bogotá's microzoning [27]. The soils reported consist mainly of clays of high compressibility. Following Terzaghi's recommendations [116], the original results found in the microzonation study were modified by grouping stratums that shared similar geotechnical characteristics as unit weight and undrained shear strength, obtaining at most six soil layers. Table 3.2 summarizes the geotechnical properties for each BH (denoted by N and the BH number).
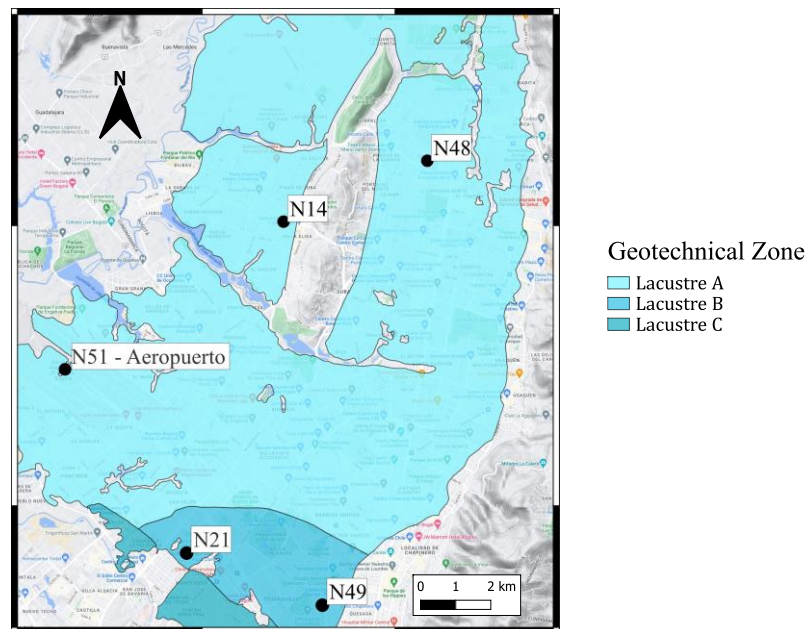
Figure 3.2 BH location

The foundation elements of the MRF building comprise caps supported by reinforced concrete (RC) piles, while the thin-walled building utilizes a strip footing resting on RC piles to transfer the superstructure loads to the soil. The cross-sections of both the caps and strip footing were designed with dimensions set to twice the diameter of the pile for the base and 1.5 times the pile diameter for the height. The dimensions of the piles (see Table 3.3) were selected to ensure that both the shaft and tip bearing capacities, calculated using the alpha method (recommended for

cohesive soils) [117] and the Hansen equations [118], respectively, were able to withstand the loads transferred by the superstructure. The design aimed for an efficiency of at least 90% in load-bearing capacity.

Table 3.2 Design soil profiles and foundation dimensions. γ: unit weight and Su: undrained shear strength.

BH	Stratum	Depth [m]	γ [kN/m³]	Su [kPa]
	1	7.0	13.9	29.5
	2	9.0	12.5	15.0
	3	14.0	13.0	9.0
N14	4	23.0	12.6	14.0
	5	29.0	13.9	9.5
	6	40.0	12.6	23.0
	1	8.0	15.3	43.3
	2	14.0	16.0	32.5
	3	18.0	14.0	40.0
N21	4	24.5	13.3	20.0
	5	30.0	14.0	45.0
	6	40.0	18.0	50.0
	1	12.0	13.7	24.4
	2	23.0	13.2	13.5
N48	3	32.0	14.6	27.5
	4	43.0	13.3	31.6
	5	50.0	13.9	27.5
N49	1	7.0	16.8	45.0

BH	Stratum	Depth [m]	γ [kN/m³]	Su [kPa]
	2	16.0	13.5	15.0
	3	22.0	14.0	30.0
	4	40.0	16.4	45.0
	1	7.0	13.7	24.4
	2	14.0	13.2	13.5
	3	21.0	14.6	27.5
N51	4	25.0	13.3	31.6
	5	30.0	13.9	27.5
	6	37.0	13.7	26.0

Table 3.3 Piles dimensions

BH	Bearing Stratum	Su [kPa]	MRF building		Thin walls building	
			D [m]	L [m]	D [m]	L [m]
N14	6	23.0	0.6	35.0	0.6	40.0
N21	6	50.0	0.5	35.0	0.5	35.0
N48	4	31.6	0.5	35.0	0.6	40.0
N49	4	45.0	0.5	35.0	0.5	35.0
N51	6	26.0	0.5	35.0	0.6	35.0

3.2.2   Nonlinear modeling of the structure

3.2.2.1   Superstructure

3.2.2.1.1 Frame building

The building was modeled in 2D using OpenSees software with the distributed plasticity approach. Modeling the structures in 2D entails a reduction in computational effort specially when

the substructure is considered. The chosen frame corresponds to frame number 3 (Figure 3.1a since it corresponds to the frame with the largest tributary area. Structural elements (beams and columns) were modeled using ForceBeamColumn element and a fiber approach [85] was applied to consider the action of the unconfined and confined concretes, and the reinforcement steel materials. Five integration points were used distributed along each element and a Gauss-Lobatto integration scheme [119] was chosen to compute the forces and stresses produced in each structural element. P-delta effects were captured for the columns by applying the PDelta transformation available in Opensees. The model uses 3% of damping as suggested by Deierlein *et al*. [93]. Additionally, rigid diaphragms on each floor were formed by means of EqualDOF constraint, which imposes the displacements experienced by a master node to slave nodes.

The confined and unconfined concretes were modeled using the Kent-Scott-Park zero tensile Concrete01 material [120], where the properties of the former were computed based on the Mander model [86]. The reinforcement steel was modeled using a uniaxial bilinear Hysteretic material which properties are based on the report of Carrillo *et al.* [88]. The reinforcement steel backbone was modified applying the MinMax material model [89] to capture the steel rupture and buckling. The MinMax restrains the strains that a material can undergo, so once such limits are surpassed the material stops functioning. For this study such limits were set to -0.008 for buckling that comes after the spalling of the concrete [121] and to 0.05 to account for the low cycle fatigue [90]. For concrete, a regularization technique based on the constant fracture energy [122] was applied to the structural elements based on the length (L), elasticity modulus (E) and fracture energy (Gf). The elasticity modulus was calculated using Equation 3.1 [123] and the fracture energy was set to the peak strength for unconfined concrete and to twice the peak strength for confined concrete. The regularization is considered by means of a strain which was taken as the ultimate strain for the

concrete constitutive models. Table 3.4 and Table *3.5* show input parameters for both materials and Figure 3.3 depicts the backbone curves.

$$E = 4300\sqrt{f'c} \qquad \text{Equation 3.1}$$

Table 3.4 Input parameters for Concrete 01 material

	fpc	epsc0	fpcu	Beam L = 6m	Beam L = 7 m	Columns
				epsU		
Confined	28.0	0.002	5.6	0.007	0.006	0.012
Unconfined	36.4	0.003	7.3	0.012	0.011	0.024

Table 3.5 Input parameters for Hysteretic material

s1p	e1p	s2p	e2p	s3p	e3p
443	0.0029	545.7	0.1026	4.4	0.1
s1n	e1n	s2n	e2n	s3n	e3n
-443	-0.0029	-459.4	-0.1026	-4.4	-0.1
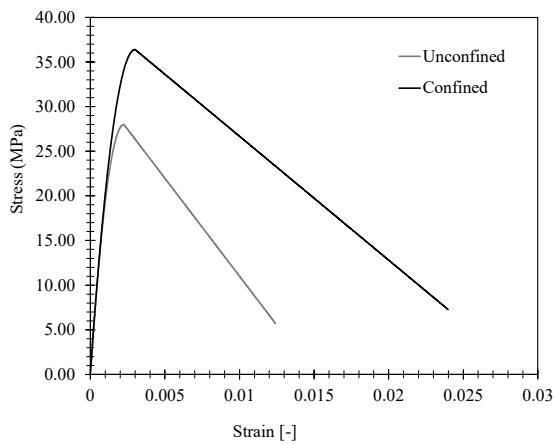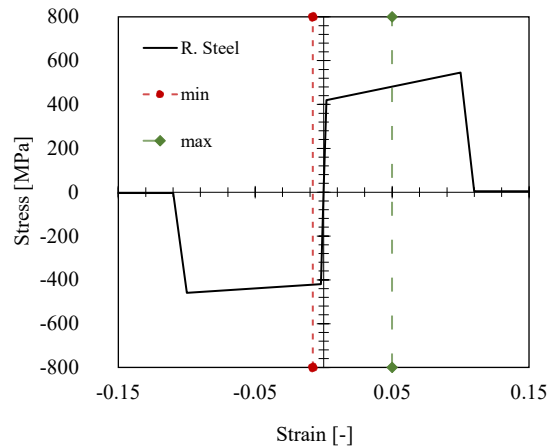
(a)   (b)

Figure 3.3 Materials backbone curves for frame building model. (a) Concrete; (b) Steel bars

3.2.2.1.2 Thin-Walls building

The RC walls were modeled in Opensees by means of the multiple-vertical-line-element-model (MVLEM) [115]. In such model, the wall is simulated by a series of macro-fibers elements connected to rigid beams at the top and at the bottom of the element. The flexural and shear responses are uncoupled, and the shear response is described by a spring located at a given height (ch), herein taken as 0.4 as recommended by Vulcano *et al.* [124]. For this study, the walls modeled correspond to those highlighted in black in the plan layout in Figure 3.1(b). hese particular walls were selected as representative in the longitudinal direction following a pushover analysis, which determined that they absorbed the highest percentage of base shear for the building. The walls were discretized using 14 macro-fibers to which reinforcement steel and concrete properties were assigned. The model has rigid diaphragms at every floor represented by the EqualDOF command applying a constraint in the x direction.

Since the building reinforcement corresponds to a welded-wire-mesh longitudinally arranged, the confinement effect is not present, so the materials assigned to each macro-fiber are unconfined concrete and steel reinforcement. The backbone of each material is presented in Figure 3.4. The concrete was modeled using Concrete01, where the concrete crushing strength was assumed as 10% of the concrete compressive strength. The Hysteretic material was used to model the WWM reinforcement, using the properties described by Carrilo *et al.* [125] for WWM reinforcement. The MinMax material was applied using strain limits of -0.006 [126] and 0.0186, which corresponds to the fracture strain for the WWM. In the case of the elastic material used to model the shear behavior of the wall, the shear modulus for the concrete in the section was considered as 40% of the concrete elasticity modulus, which was calculated using Equation 3.1.

(a)

(b)
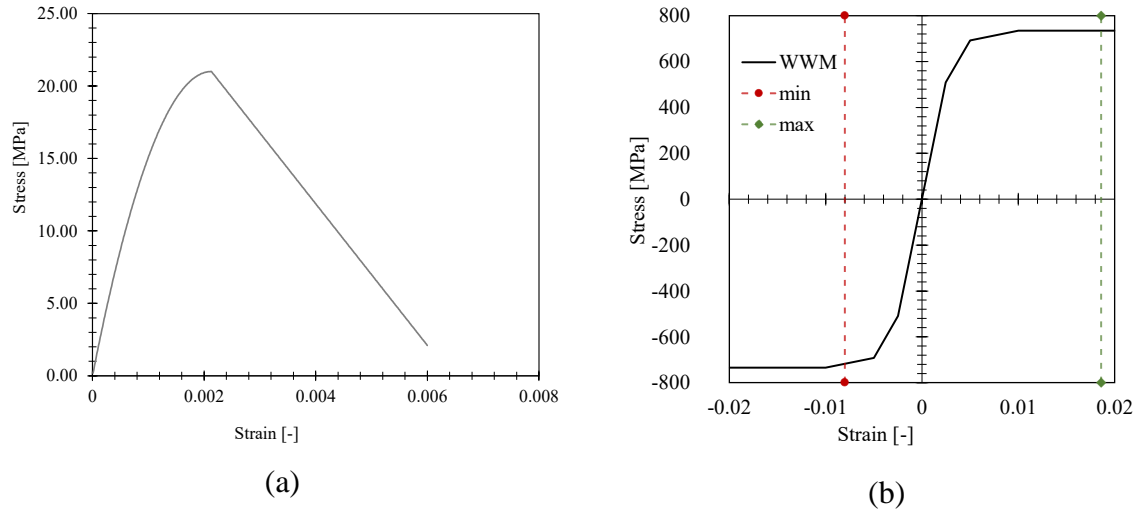
Figure 3.4 Materials backbone curves for thin walls building model. (a) Concrete; (b) Welded-wired mesh

3.2.2.2 Foundation

For the foundation modeling an equivalent foundation was calculated to be representative of the building. The pile spacing was set to three times the pile diameter to mitigate the stress bulbs overlapping. The foundation modeling considered two conditions: the first one consisted of the fixed base (common practice) and the second one a flexible base approach. The first approach is addressed by fixing the degrees of freedom of the base nodes. For the second approach, piles and caps were modeled using the elasticBeamColumn element with linear properties based on the Young's Modulus (Equation 3.1) for a compressive strength of 28 MPa) and the section moment of inertia. Additionally, as for the columns in the superstructure, the PDelta transformation was applied to the piles, and the caps were considered as beams, which use the Linear transformation.

3.2.2.2.1 SSI modeling

The soil-structure modeling considers two soil states: linear and nonlinear. The linear modeling consists of a layered Winkler-type medium [127], assumed to behave linearly whereas the nonlinear approach uses the Beam on Nonlinear Winkler foundation (BNLWF) model [128].

46

In both cases, the soil was modeled as one-dimension springs that are distributed along the interface of the soil-foundation system. The spring spacing was closer in the upper soil layers until the active pile length (twenty times its diameter) in order to obtain a better representation of the pile-soil interaction in the structural analyses [18]. Figure 3.5 shows an example of a foundation. The horizontal components symbolize the pile caps, while the vertical components represent the piles. These elements are interconnected through a sequence of nodes that also link the springs with the substructure.
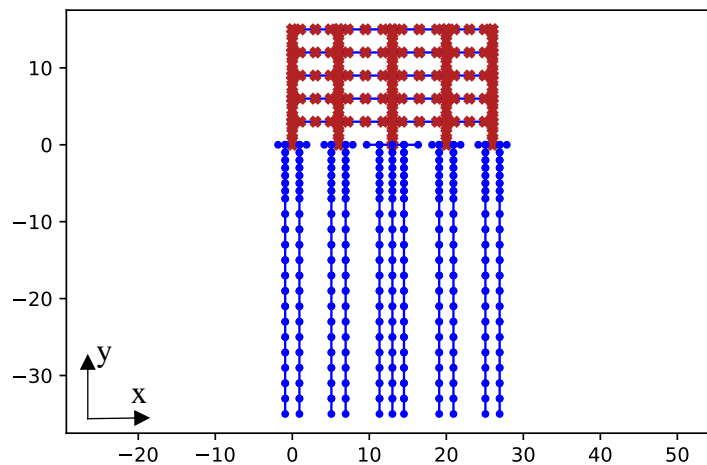
Figure 3.5 Example of substructure node distribution for RC frame case BH 14

Linear approach

The linear approach modeling uses zeroLength elements available in OpenSees, which links two nodes in the same location by multiple UniaxialMaterial objects. This study considers two cases: one with springs in the vertical direction (Figure 3.6a) and the other with springs in both, vertical and horizontal directions (Figure 3.6b). The linking nodes were the pile nodes and a neighboring node with the same coordinate as the pile one but was completely fixed to simulate boundary conditions. The linking material used corresponds to the Elastic UniaxialMaterial with a tangent value set to the lateral subgrade modulus of soil (K), computed using the Equation 3.2

proposed by Bowles [19]. Such expression relates the undrained shear strength (Su) and simulates a failure state condition.

(a)   (b)

Figure 3.6 zeroLength linear approach spring configuration. (a) springs in both directions, (b) springs in the vertical direction.

$$K = 72Su \qquad \text{Equation 3.2}$$

Figure 3.7 shows the subgrade modulus profile for each Borehole. The subgrade reaction modulus was multiplied by the tributary area of the pile node in order to obtain its contribution per unit length. The behavior of the subgrade modulus changes in depth, showing that the upper layers exhibit larger values than those obtained for the deeper ones. The variations in the soil modulus can be attributed to the presence of a water table, which decreases the effective stresses on the soil, thereby reducing its capacity. Conversely, at depths ranging from 35 to 40 meters, the soil strength increases due to the process of consolidation experienced by the material. Additionally, the profiles can be useful to identify the locations with the best and poor soil conditions. For instance, the N14, N48 and N51 boreholes present remarkably low and similar subgrade modulus; all of them belong to the Lacustre A geotechnical zone, which spreads in the north, north-west and west of Bogotá (see Figure 3.2).
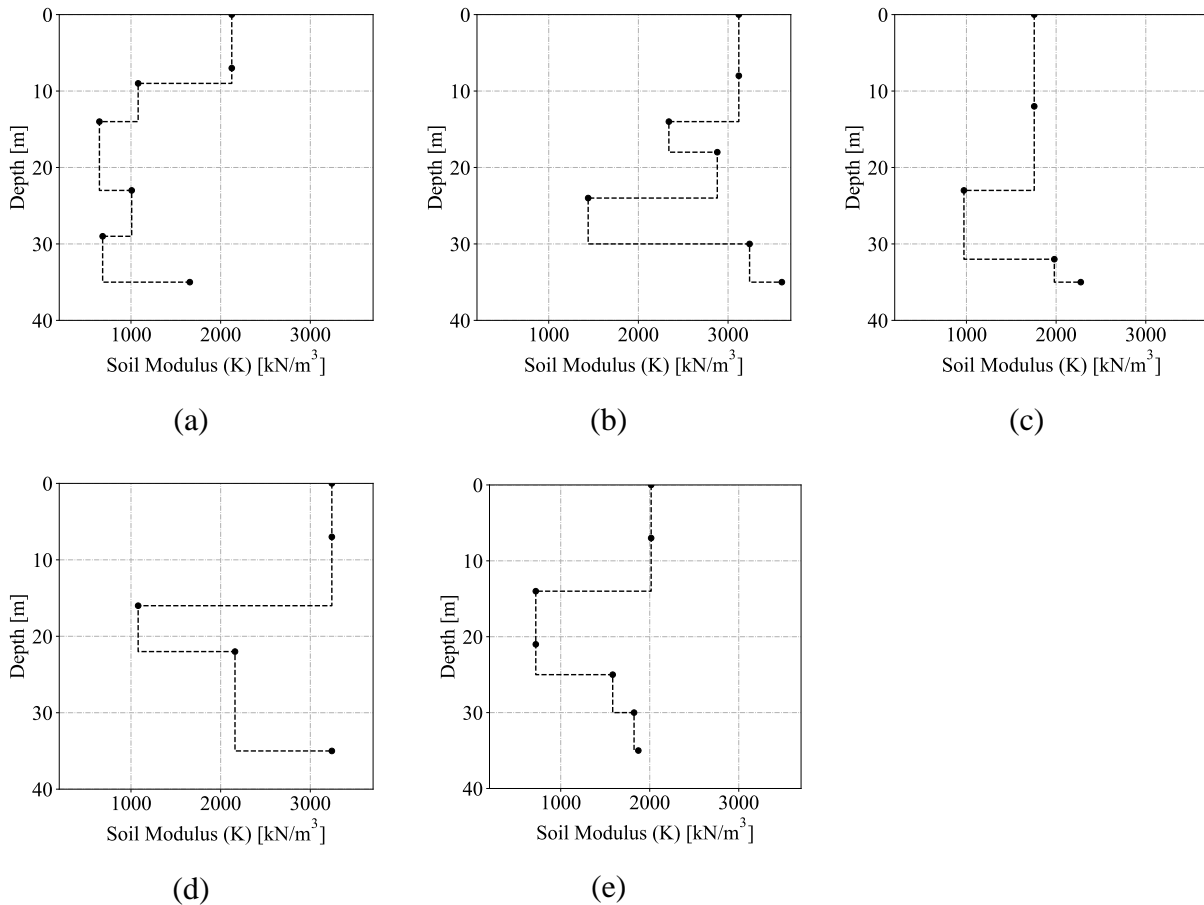
Figure 3.7 Subgrade reaction modulus profiles. (a) BH-14, (b) BH-21, (c) BH-48, (d) BH-49, (e) BH-51

Nonlinear approach

Likewise the linear approach, zeroLength elements were used to model the soil-pile interaction but in this case the linking elements used were the PySimple1 [129], TzSimple1 [130], and QzSimple [131] for the horizontal and vertical springs, as depicted in Figure 3.8. The materials are defined in Opensees in accordance with the study of Boulanger *et al*. [17], who calibrated the behavior of these materials with deep foundation tests. The springs are conceptualized as a series of elastic, plastic, and gap (drag and closure) springs along with a dashpot placed in the elastic one. The elastic material describes the "far-field" behavior, while the plastic component represents the "near-field" permanent displacements. The p-y spring models the passive pressure that the soil

49

experiments under horizontal loading, t-z spring captures the slippage on the foundation in the soil due to the vertical load that comes from the superstructure, and the q-z spring accounts for the tip bearing capacity.
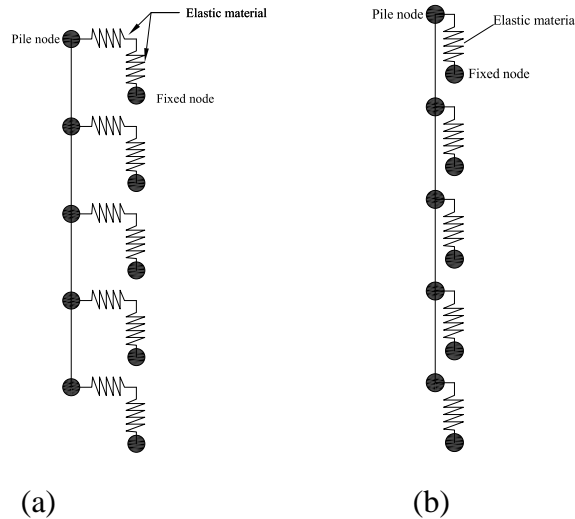

(a)   (b)
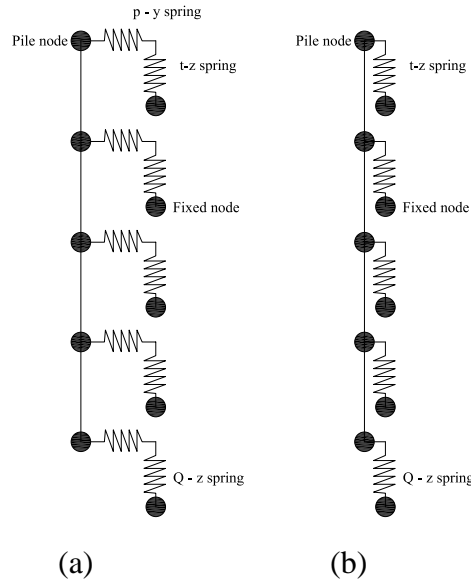
Figure 3.8 zeroLength non-linear approach spring configuration. (a) springs in both directions, (b) springs in the vertical direction.

The parameters that condition the behavior of the PySimple1 material (p_{ult} and y_{50}) were computed based on Matlock's equations for soft clays [132] as follows:

$$p_{ult} = C_u B N_p \qquad \text{Equation 3.3}$$

Where, C_u is the undrained shear strength, B is the pile diameter and N_p corresponds to a lateral bearing capacity factor that was defined as 2.5 for depths lower than five times the pile diameter and 11 for greater values since the lateral bearing capacity of soils increases with depth.

$$y_{50} = 2.5 B \varepsilon_{50} \qquad \text{Equation 3.4}$$

Where, ε_{50} is the strain corresponding to 50% of the ultimate stress in a laboratory stress-strain curve. The TzSimple1 and QzSimple1 materials represent the ultimate skin and tip resistance

50

of the pile that were calculated using the equations Equation 3.5 [133] and Equation 3.6 [118], and

the z_{50} for both cases were calculated by the equations Equation 3.7 and Equation 3.8 found in

Harden [134] for the clay-case. Such equations use an equivalent stiffness (K) in the vertical

direction that was defined as the subgrade modulus, following the recommendations of the

American Petroleum Institute (API) [135].

$$t_{ult} = A_s C_u \quad \text{Equation 3.5} \qquad\qquad q_{ult} = 9A_t C_u \quad \text{Equation 3.6}$$

Where, A_s and A_t are the skin friction and tip areas of the pile.

$$z_{50} = \frac{0.708 t_{ult}}{K} \quad \text{Equation 3.7} \qquad\qquad z_{50} = \frac{0.525 q_{ult}}{K} \quad \text{Equation 3.8}$$

The damping used in the models was set to 3%, which is the value for the viscous damping

calculated in the microzoning project and then supported by Suarez [136] in her study of the

dynamic parameters of the Bogotá clayey soils.

3.2.3 Nonlinear analysis

3.2.3.1 Pushover

A pushover analysis is mainly used to estimate how far into the inelastic range a building

can go until reaching partial or total collapse [137]. This is reached by means of applying a load

pattern to the building to simulate the ground motions. In this case, an inverted triangular pattern

was used. The analysis configuration is as follows: displacement control integration scheme with

0.001 mm steps until a target displacement of 2% and 3% of the roof drift was reached for the

MRF and thin-walled structures, respectively. A plain approach was applied to handle the

constraints of the model. Additionally, the Reverse Cuthill McKee (RCM) numberer object was

selected for numbering the degrees of freedom of the structure since the method allows to reduce the bandwidth of the structure stiffness matrix. The EnergyIncrement convergence test with a tolerance of 1×10^{-8} was considered. For this analysis, the linear and nonlinear soil modeling conditions were accounted.

3.2.3.2 *Fragility Analysis*

The fragility analysis was conducted by a time history analysis [138]. The ground motions selected for this analysis consisted of the 3,140 signals generated for Bogotá within the framework of the National Seismic Risk Model, considering the city's seismic hazard with the conditional scenario spectra methodology [139]. In this analysis, the integrator chosen for the models with linear soil modeling was Newmark, while those with soil nonlinearity used the Hilber-Huges-Taylor method, as recommended by OpenSees documentation [129]. The time step used for the analysis was the same as the ground motion.

The structural damage was assessed by means of inter-story drift ratios. The exceedance of four damage states was measured, i.e., slight, moderate, extensive and collapse. The reference values for inter-story drift ratio in the RC moment-resisting frame (MRF) building were set based on [140] as follows: 0.33%, 0.58%, 1.56%, and 4.00% for each respective damage state. In the case of thin walls, structural damage assessment was conducted using roof drift as the engineering demand parameter (EDP). The threshold values for each damage state were defined separately for the fixed and flexible base models following the procedure proposed in the National Seismic Risk Model of Colombia for the thin-walled structures. The procedure consists of plotting the results of the EDP against the intensity measure. This allows for the identification of the numerical instability point in the results, which is taken as the collapse of the structure. The evaluation involves analyzing the slope of the median data, and when a significant change in slope is observed, a cut-

off line is drawn on the y-axis. The corresponding EDP value on this line is considered to be the point at which the structure fails (see Figure 3.9).
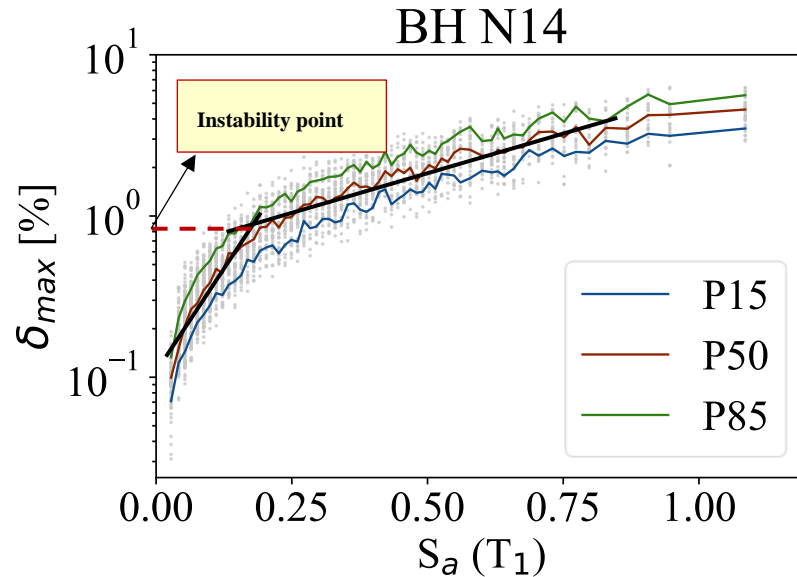
Figure 3.9 Numerical instability determination procedure

The values for the fixed base were 0.04%, 0.24%, 0.36%, and 0.50%, which were defined within the MNRS framework. Regarding the flexible base, the values were carefully determined to maintain the same relationship between each damage state as observed in the fixed base approach. Consequently, the resulting values for the flexible base were established as 0.035%, 0.17%, 0.31%, and 0.43%.

The resulting curves were adjusted to a lognormal distribution following the procedure recommended by Baker [141]. As this analysis uses dynamic loads, only the nonlinear approach was analyzed since the consideration of the subgrade modulus in this kind of analysis can lead to significant underestimation of soil stiffness and overestimation of the amount of displacement and rotation experienced by the structure [142]. In addition, the fragility curves were computed only for the models that considered the soil in x and y directions.

3.3 Results and Discussion

The structural periods in Figure 3.10 show the effect that including the foundation and soil induces in the stiffness of the buildings. The MRF (Figure 3.10a) structure period increases by 20% when the soil is considered in both directions with nonlinear properties. Furthermore, it is evident that the subgrade characteristics has a significant influence on the structural periods. Particularly, in the cases where the bearing capacities of the soil stratums were low, there was an increase in the structural periods. For the thin walls (Figure 3.10b), the period increases three times compared to the fixed base model. The findings further underscore the impact of the foundation dimensions on the modal response, as stiffer foundations result in lower structural periods. This relationship is particularly significant due to the strong dependence of substructure stiffness on the pile diameter and length.
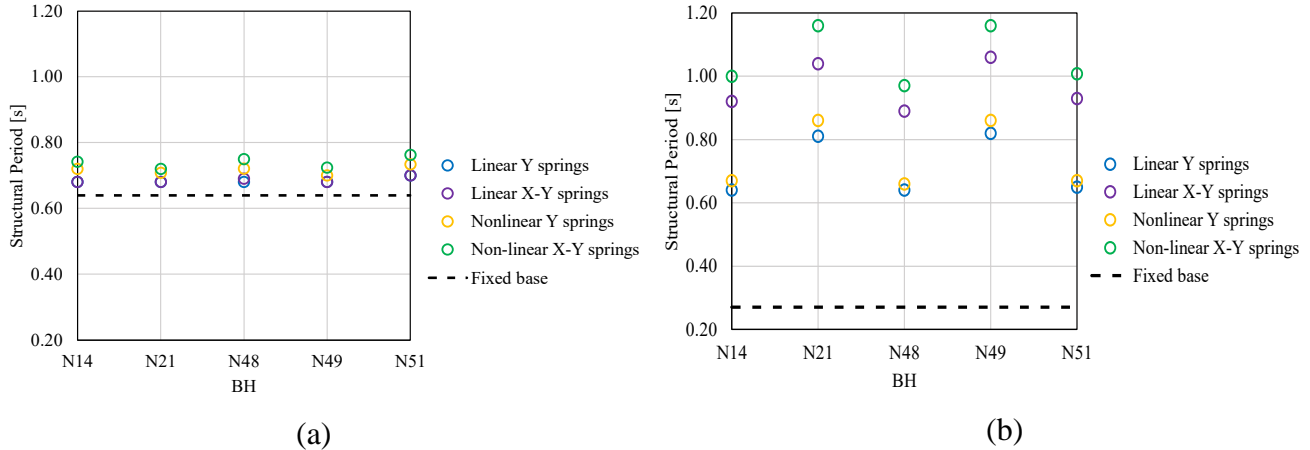
Figure 3.10 Reported structural periods. (a) MRF Building and (b) Thin walls building

Figure 3.11a depicts the relationship among the building's structural periods, the bearing capacity of the piles, and the foundation stiffness (represented by the size of the bubble). The findings are coherent with the previously mentioned remarks for both buildings. The bubbles distribution observed in the MRF building enhance the significant influence of soil characteristics

on the system stiffness. When the soil foundation corresponds to BH with lower bearing capacities (i.e., N14, N48 and N51), the structural stiffness decreases, resulting in longer periods compared to those obtained with higher bearing capacities (i.e., N21 and N49).

Conversely, Figure 3.11 b reveals a stronger dependence of the thin-walled structure on the foundation stiffness. Irrespective of the soil type, the building periods decrease as the foundation stiffness increases. This highlights that the stiffer the foundation, the shorter the building periods for the thin-walled structure.

(a)

(b)
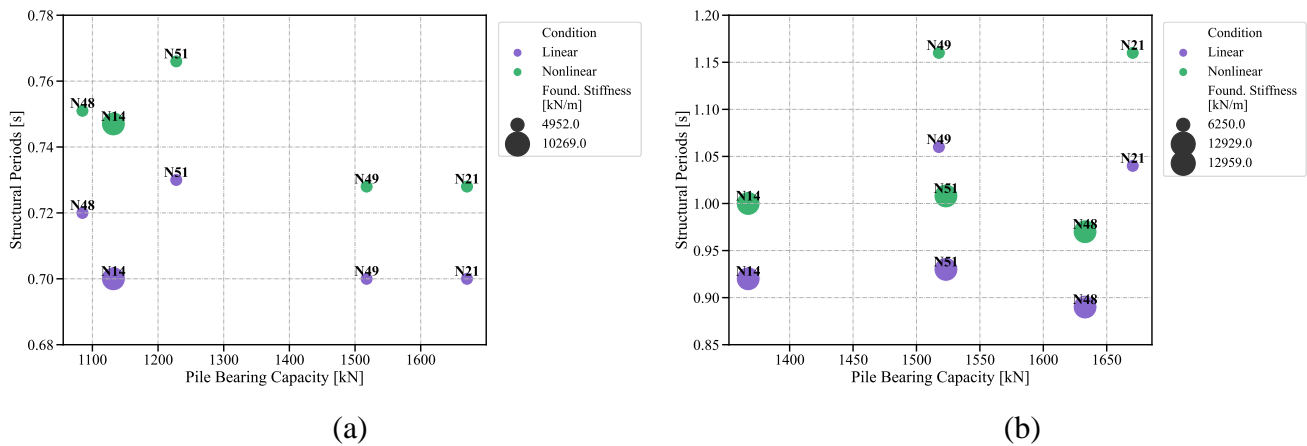
Figure 3.11 Structure-substructure-soil relationship. (a) MRF building and (b) Thin walls building

Figure 3.12 shows the capacity curves for both structural systems considering fixed and flexible base. Various highlights can be obtained from these results. There are remarkable differences between the seismic performance of both structural systems, since the flexible base seems to have a higher effect in the thin-walled structure than the MRF structure. Such condition can be attributed mainly to the stiffness difference existing among the superstructure and the substructure. The capacity curves from the models that consider the flexible base shows a change on the stiffness of the system, which is confirmed with the structural periods in Figure 3.10.

The pushover analysis also highlights the impact of soil modeling approach (linear or nonlinear) on the seismic response of the building. For the MRF system (Figure 3.12a-1 to Figure 3.12e-1), when linear soil properties are considered, the capacity curve slightly shifts to the right, indicating lower stiffness compared to the fixed base model. In contrast, nonlinearity in the soil results in decreased stiffness relative to both the fixed base and linear approaches. However, including the foundation in the analysis does not significantly alter the base shear experienced by the MRF building. In the case of RC walls (Figure 3.12a-2 to Figure 3.12e-2), the modeling approach for the soil springs affects the behavior of the building, leading to higher roof displacements and slightly higher base shear values when the flexible foundation is considered with the soil modeled in both the x and y directions for all the BH studied. Additionally, the pushover results emphasize the effect that the nonlinearity of the soil exerts in the building's lateral capacity, which is further studied by obtaining the system ductility values.

(a-1)   (a-2)

(b-1)

(b-2)

(c-1)

(c-2)

(d-1)

(d-2)

(e-1)
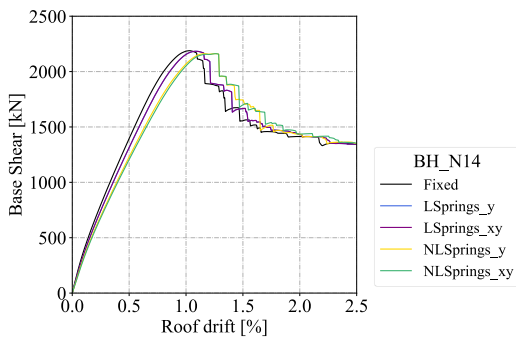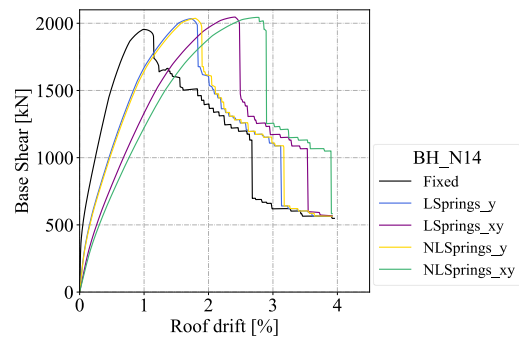
(e-2)
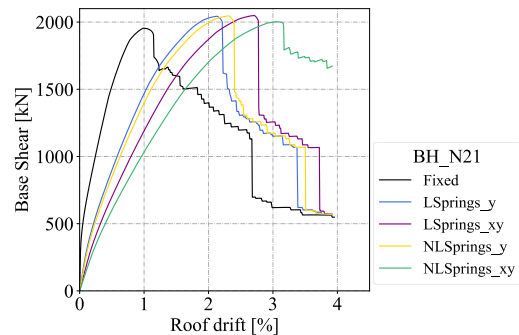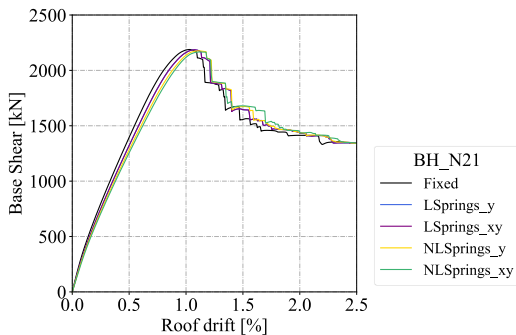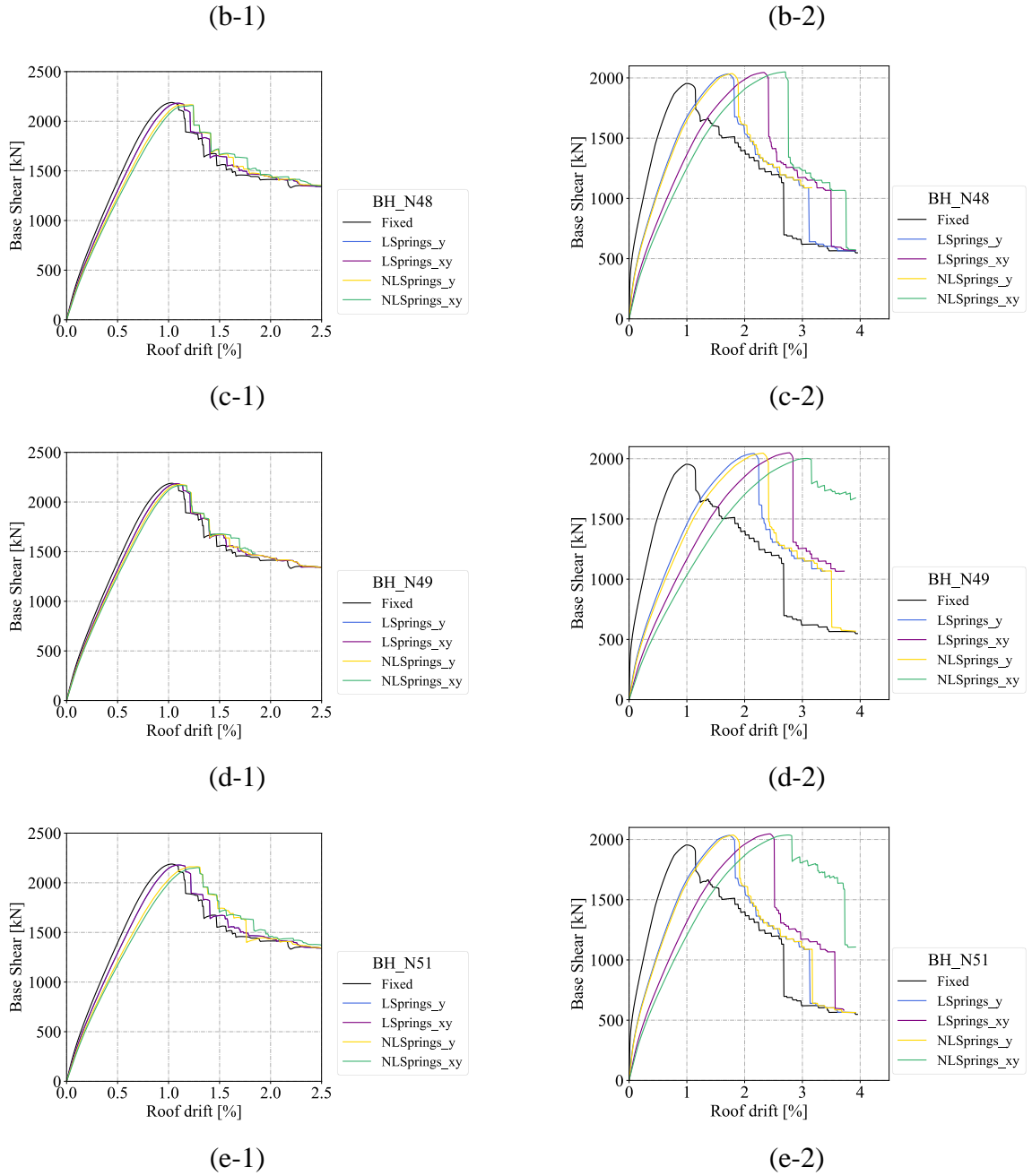
Figure 3.12 Capacity curves. (a) BH N14, (b) BH N21, (c) BH N48, (d) BH N49, and (e) BH N51

The buildings ductility was computed using the Equation 3.9.

$$\mu = \frac{u_{80}}{u_y} \qquad \text{Equation 3.9}$$

Where, u_y is the yield displacement and u_{80} the displacement at which the building capacity drops to 80% of the maximum. Table 3.6 summarizes the ductility results for MRF and thin walls buildings. In the case of the thin-walled structure, a significant reduction in ductility is observed. When considering linear soil characteristics, the ductility decreases from 4.0 (with fixed base) to values ranging between 2.4 and 2.6. When nonlinear characteristics are taken into account, the ductility ranges between 2.6 and 3.3. These findings highlight the sensitivity of the thin-walled structure to soil conditions, with nonlinear characteristics resulting in slightly improved ductility compared to linear characteristics.

The ductility of the MRF building also experiences a reduction for some of the studied BH, although to a lesser degree. Under linear soil characteristics, the ductility decreases from 2.7 to a minimum value of 2.4, while under nonlinear characteristics, it reaches a minimum of 2.2. However, a different trend is observed for the N14 BH, where the ductility of the building remains unchanged under linear soil conditions and increases under nonlinear soil conditions. Overall, the MRF building demonstrates a relatively higher resilience to changes in soil conditions compared to the thin-walled structure. Furthermore, a general trend is observed, indicating slightly higher ductility values for BH with lower bearing capacities.

The changes in ductility for both types of buildings indicate that although the structures can withstand larger roof displacements when considering soil-structure interaction (SSI), their capacity of deformation before reaching failure diminishes. Notably, most of the capacity curves obtained show a sudden decline after a certain roof displacement, suggesting that the structures have experienced significant load-carrying capacity and may even be on the verge of critical failure or collapse.

Table 3.6 Ductility values

Fixed Base		BH	Linear		Nonlinear	
MRF	Thin Walls		MRF	Thin Walls	MRF	Thin Walls
		N14	2.7	2.5	3.2	2.7
		N21	2.4	2.5	2.2	2.7
2.7	4.0	N48	2.5	2.4	2.4	2.6
		N49	2.4	2.6	2.3	3.3
		N51	2.5	2.5	2.4	3.2

These findings indicate that the influence of soil-structure interaction (SSI) may be less significant in flexible structures like MRF buildings compared to more rigid structures such as thin-walled buildings. This behavior can be attributed to the substantial disparity in stiffness between the superstructure and substructure.

Regarding the dynamic analysis, the median inter-story drifts are presented in Figure 3.13 and Figure 3.14 for the MRF building and thin walls, respectively. Different trends are observed in the results obtained for each group of Bore Hole (BH) analyzed, i.e., relatively low, and better bearing capacities. The box plots for BH N14, BH N48 and BH N51 (Figure 3.13b, d, and f) reveal that the higher median drift values are primarily concentrated in the second and third stories. The presence of outliers indicates that certain values deviate significantly from the norm in the analysis. This behavior is consistent across all stories, with the first, second, and third stories exhibiting more distant outliers. The results also reveal that with lower bearing capacities in the subgrade, the building yields higher values of inter-story drifts.

Turning to BH N21 in Figure 3.13c, the results suggest that the median drift values obtained from the dynamic analysis exhibit greater dispersion compared to the BH N14 case. The second

story stands out as having the largest dispersion, followed by the third story. It is worth noting the presence of numerous outliers, indicating that unusual values were computed for certain ground motions. Furthermore, the median values obtained for BH N21 are lower compared to those obtained when the subgrade characteristics correspond to BH N14. The results for the BH N49 shown in Figure 3.13e holds strong similarities to the observed in the BH N21. In general, the median drifts align with the expected distribution for MRF buildings, with larger values typically observed in the middle stories.

Upon comparing the results between the flexible base and fixed base approaches, a notable difference becomes apparent in the number of outliers. The fixed base model exhibits a considerably higher count of outliers compared to the flexible base model. Moreover, the overall behavior of the building aligns with the observed trends in the studied BHs, with one exception being the N14 case.

(a)

(b)

(c)

(d)

(e)

(f)
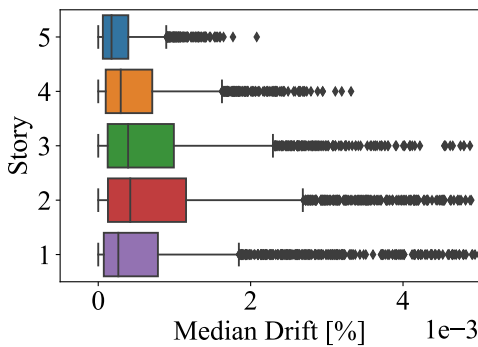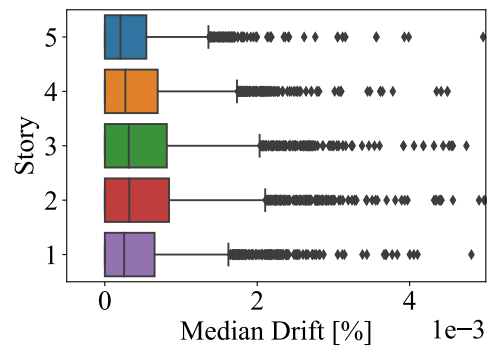
Figure 3.13. Story median drifts distribution for the MRF building. (a) Fixed base, (b) BH N14, (c) BH N21, (d) BH N48, (e) BH N49 and (f) BH N51

With respect to the results obtained for the thin-walled structure shown in Figure 3.14, the story drift distribution aligns with the typical behavior observed in RC wall structures. The boxplots generated for all the BHs exhibit a high degree of similarity for each story. It is worth noting that certain BHs exhibit a greater number of outliers in the data compared to others; however, the overall distribution of quartiles remains consistent. Additionally, it is essential to analyze the magnitude of the outliers and their potential impact on the overall data interpretation. Outliers may indicate extreme or atypical behavior in specific foundation conditions. By examining the specific characteristics of the outliers, valuable insights can be gained into potential vulnerabilities or exceptional performance within the thin-walled structure.

Overall, the consistent quartile distribution across BHs suggests a general pattern of story drift distribution, indicating a robust behavior of the thin-walled structure in response to seismic loading. However, the presence of outliers emphasizes the effect that exerts the characteristics considered in the SSI analysis. On the other hand, when the results are compared to those obtained with the fixed base model (Figure 3.14a), the incidence in the numerical results that the SSI has in the dynamic analysis is more evident as the atypical response values disappear when the building base is considered to be fixed.

(a)

(b)

(c)

(d)

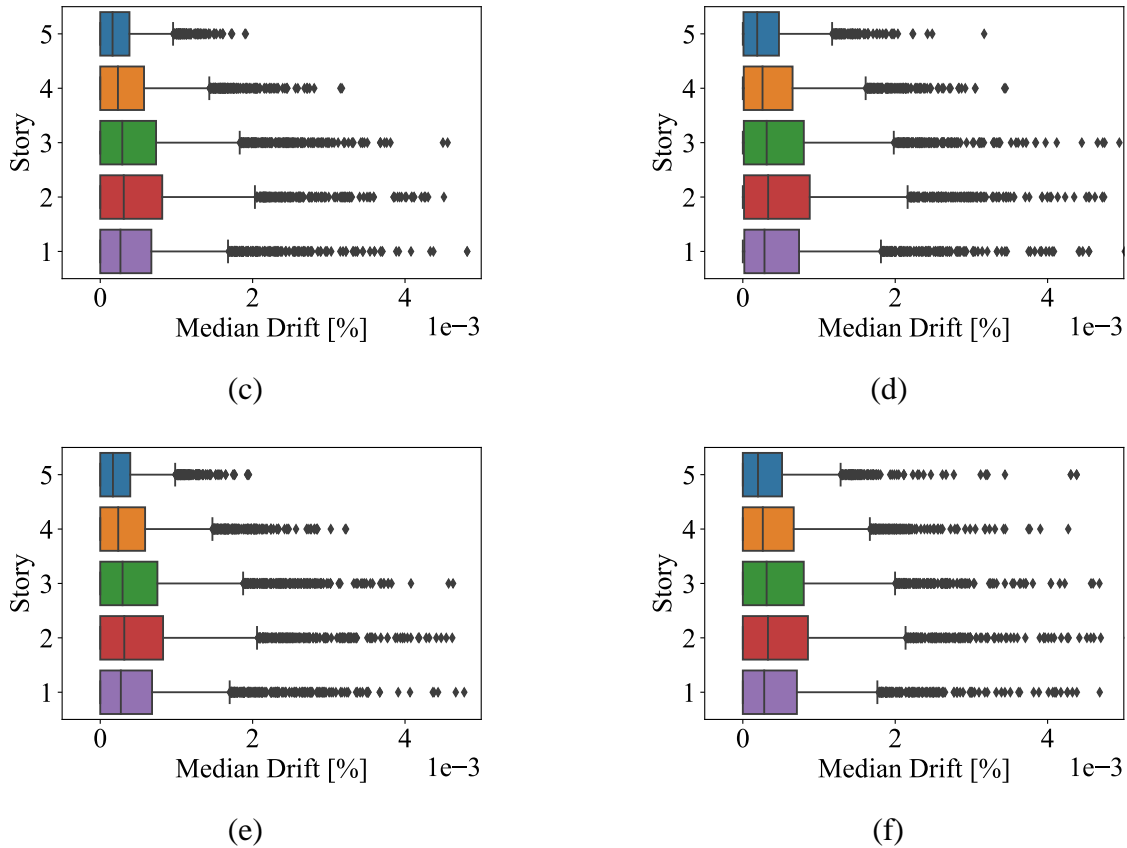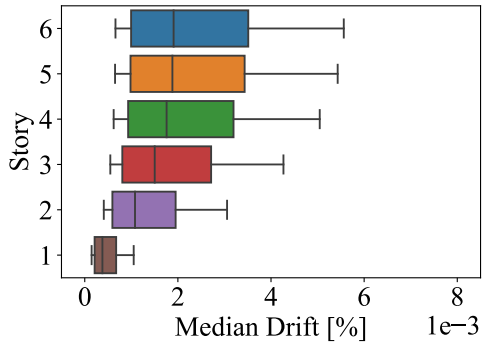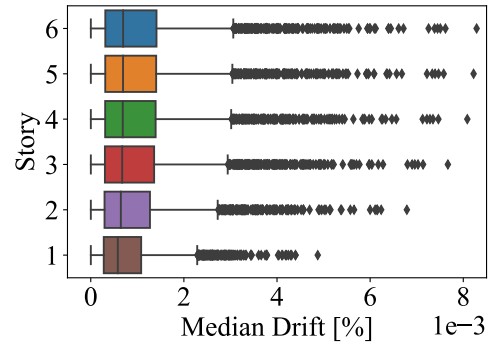(e)   (f)
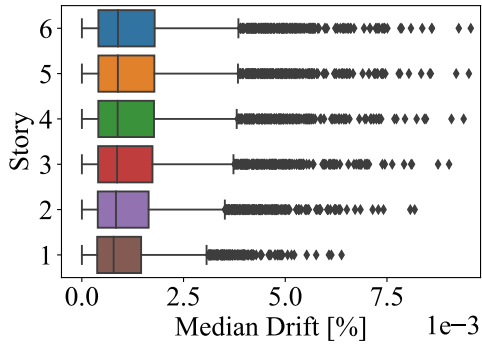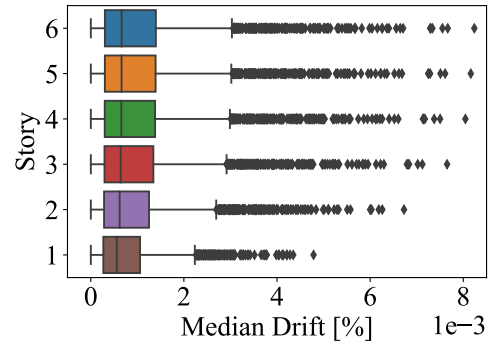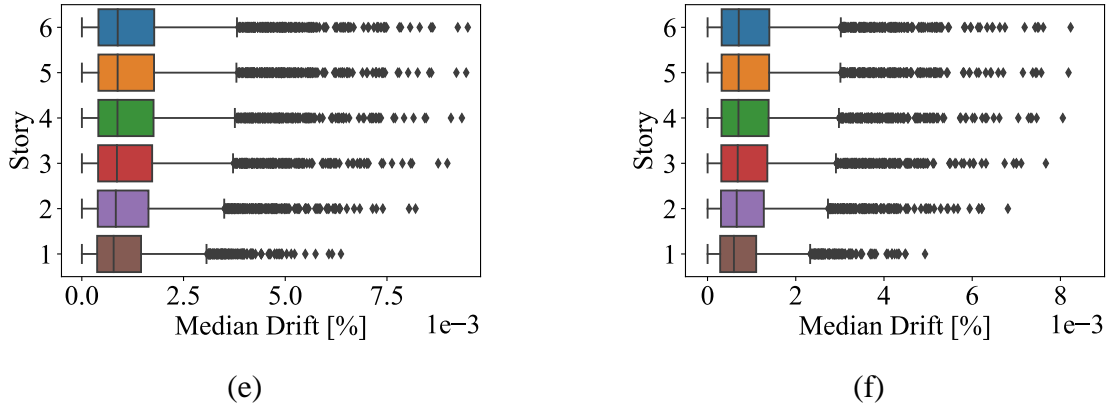
Figure 3.14 Story median drifts distribution for the thin walls building. (a) Fixed base, (b)
BH N14, (c) BH N21, (d) BH N48, (e) BH N49 and (f) BH N51.

Figure 3.15 presents the fragility curves for the RC MRF building. The findings show that

incorporating SSI in the dynamic analysis results in an increased probability of exceed the four

damage states assessed at lower intensities. Table 3.7 and Table 3.8 relate the statistical parameters

obtained from the curve fitting following the procedure proposed by Baker [141]. The tables

present the median of the fragility function and (θ) and the standard deviation (β). The influence

of SSI is evident in the changes observed in the median probabilities. These changes are

particularly notable in the extensive and collapse cases, where the intensity measure at which the

median probability of reaching such conditions increases by approximately 14% to 20% and 35%

to 40%, respectively, when compared to the fixed base scenario. For the slight and moderate

damage states, the increments are comparatively lower, ranging from 7% to 10% for the slight case

and ranging from 9% to 11% for the moderate case. Changes in the fragility response from one

BH to another are negligible and this can be confirmed by comparing the statistical parameters.

Table 3.7 Statistical parameters from curve fitting for fixed base models

	MRF		Thin walls	
DS	Beta	Theta	Beta	Theta
Slight	0.30	0.23	0.28	0.13
Moderate	0.33	0.38	0.20	0.39
Extensive	0.40	1.05	0.27	0.51
Collapse	0.55	1.75	0.29	0.66

Table 3.8 Statistical parameters from curve fitting for both buildings considering SSI

		MRF		Thin walls	
BH	DS	Beta	Theta	Beta	Theta
N14	Slight	0.32	0.21	0.07	0.04
	Moderate	0.33	0.34	0.31	0.11
	Extensive	0.45	0.91	0.32	0.19
	Collapse	0.49	1.09	0.31	0.27
N21	Slight	0.32	0.21	0.08	0.03
	Moderate	0.34	0.34	0.35	0.08
	Extensive	0.43	0.85	0.34	0.15
	Collapse	0.53	1.12	0.33	0.21
N48	Slight	0.32	0.21	0.07	0.04
	Moderate	0.33	0.33	0.30	0.11
	Extensive	0.40	0.85	0.32	0.20
	Collapse	0.50	1.10	0.31	0.28
N49	Slight	0.33	0.21	0.08	0.03
	Moderate	0.34	0.34	0.35	0.08
	Extensive	0.41	0.84	0.34	0.15
	Collapse	0.54	1.12	0.33	0.21
N51	Slight	0.32	0.21	0.07	0.04
	Moderate	0.33	0.33	0.32	0.10
	Extensive	0.43	0.87	0.31	0.19

BH	DS	MRF		Thin walls	
		Beta	Theta	Beta	Theta
	Collapse	0.49	1.06	0.31	0.27

Figure 3.15 Fragility curves for the RC MRF building. (a) BH N14, (b) BH N21, (c) BH N48, (d) BH N49, and (e) BH N51

The fragility curves for the thin-walled structure (Figure 3.16) underscore the high effect that exerts including the SSI in the dynamic analysis. In contrast to the MRF structure, all damage state exceedance probabilities exhibit substantial increases compared to the fixed base model. For instance, the intensity measure at which 50% of probability to reach the slight damage decreases by a range of 71% to 76% compared to the fixed base. Similarly, for the moderate damage state, the percentages ranges from 72% to 80%. In the case of extensive and collapse damages, the intensity measure decreases by 71% and 68% respectively. This suggests that disregarding SSI in rigid structures, particularly those with significant stiffness disparities between the structure and the foundation/soil, can result in an underestimation of the system's vulnerability.
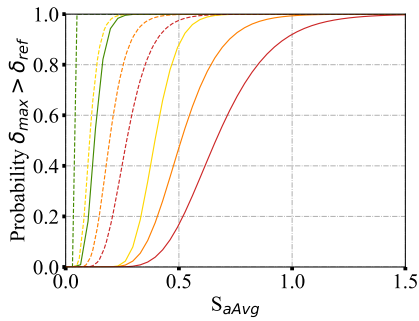
(a)
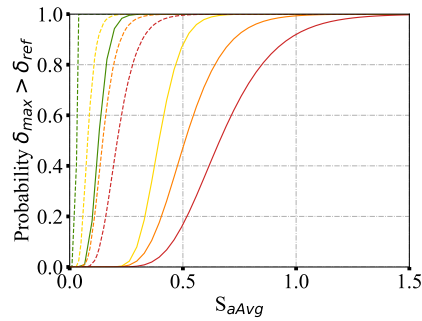
(b)
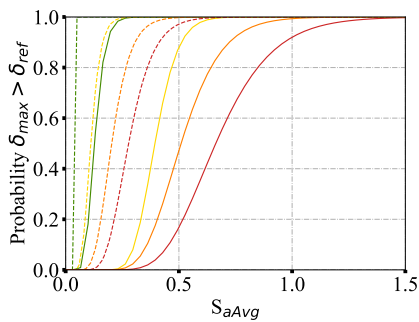
(c)
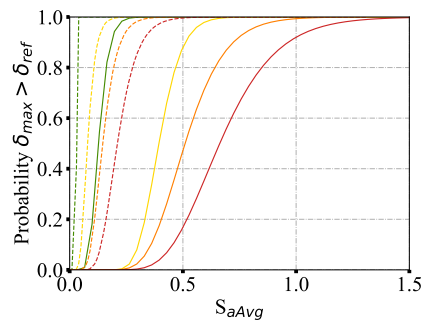
(d)
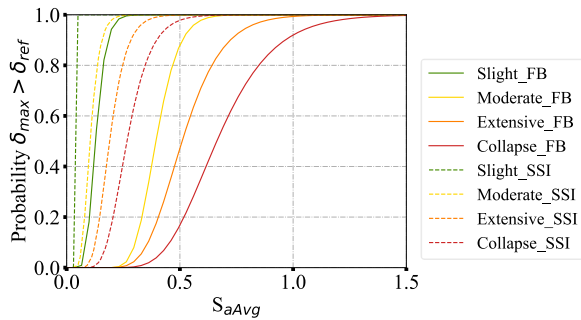
(e)

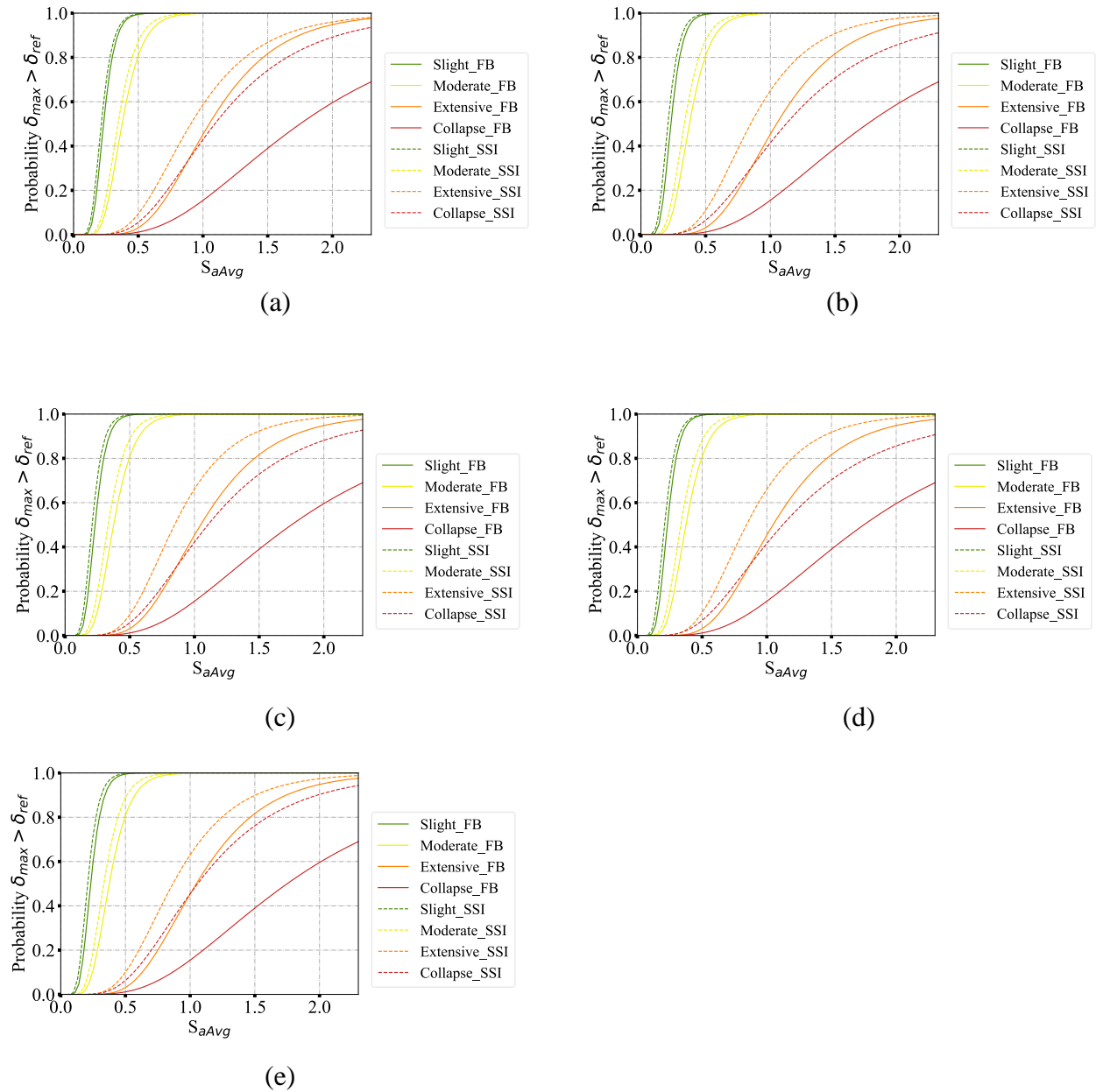**Figure 3.16** Fragility curves for the RC thin walls building. (a) BH N14, (b) BH N21, (c) BH N48, (d) BH N49, and (e) BH N51

3.4   Conclusions and future works

The seismic performance of two RC mid-rise buildings supported on deep foundations in the clayey soils of Bogotá, the capital city of Colombia incorporating soil-structure interaction (SSI) was assessed. The structural systems considered were moment resisting frames (MRF) and thin walls. Two-dimensional numerical models of the buildings were developed in OpenSees and then analyzed via Pushover and Time History Analysis. The dynamic analysis was conducted for 3 142 ground motions generated with the conditional scenario spectra for Bogotá in the National Seismic Risk Model framework. The soil was considered to behave linear and nonlinearly. The results support the following remarks:

Both structural systems exhibit differences in seismic performance when considering SSI. The MRF building experiences a 20% increase in period compared to the fixed base, with a clear dependence on the soil properties. Lower bearing capacities resulted in higher structural periods, while higher bearing capacities yield shorter periods. In contrast, the thin-walled structure shows a threefold increase in periods compared to the fixed base model. This behavior can be attributed to the substantial difference in stiffness between the superstructure and substructure. Furthermore,

67

the soil modeling approach, particularly considering nonlinear properties, has a noticeable impact on the structural responses. The observed reduction in ductility implies that although the buildings may exhibit larger lateral displacements with a flexible base compared to a fixed base, their capacity for deformation before reaching failure diminishes for both systems.

The fragility curves incorporating SSI effects, demonstrate an increase in the probability of exceeding damage states for both buildings. The fragility of the MRF building experiences a significant increase in the severe and collapse damage states, as the intensity measure at which the 50% of probability for each damage is reached, reduces by 35% and 40%, respectively. The thin-walled structure exhibits more significant changes, with increments of 76%, 80%, 71%, and 68% for slight, moderate, extensive, and collapse damage states, respectively. Furthermore, the steep slope observed in the fragility curve for the slight damage state, when considering the SSI, clearly indicates that the assessed building is highly susceptible to experiencing slight damage even at low intensity levels. These results show that neglecting SSI in fragility analyses might underestimate the vulnerability of buildings. These findings align with state-of-the-art studies conducted on similar structures, further validating the importance of considering SSI effects in seismic vulnerability assessments.

The findings of this study underscore the effect that the SSI exerts in the seismic performance of two different buildings founded on soft soils of Bogotá. To extend the findings of this study, future works could investigate the seismic performance of tall and low buildings delving into the thin walls structural system since it showed to be the more susceptible to the inclusion of the SSI. Additionally, other SSI modeling approaches can be pursued (i.e., the direct approach) or different materials to those used for this research. Recently, the PySimple1 material employed to represent the nonlinearity of soils does not include the rate-effect that can affect clays when subjected to

loading. In addition, it can overestimate the material damping at great strains as well as underestimate the pile response. To overcome such situations, future research can be addressed by implementing the PySimple5 approach proposed by Wang and Ishihara [143] that uses a genetic algorithm to adjust the material response to a specified response obtained through laboratory testing.

4   Conclusions

The findings of this work expose the importance of considering the SSI in the seismic performance analysis of the structures, mainly in those that exhibit substantial differences with respect to the foundation-soil system. Both structural systems evaluated in the research exhibit significantly different seismic performance when considering SSI. The MRF building experiences a 20% increase in period compared to the fixed base, with a clear dependence on the soil properties. Lower bearing capacities resulted in higher structural periods, while higher bearing capacities yield shorter periods. In contrast, the thin-walled structure shows a threefold increase in periods compared to the fixed base model. This behavior can be attributed to the substantial difference in stiffness between the superstructure and substructure. Furthermore, the soil modeling approach, particularly considering nonlinear properties, has a noticeable impact on the structural responses. The observed reduction in ductility implies that although the buildings may exhibit larger lateral displacements with a flexible base compared to a fixed base, their capacity for deformation before reaching failure diminishes for both systems.

The fragility curves, incorporating SSI effects, demonstrate an increase in the probability of exceeding damage states for both buildings. The fragility of the MRF building experiences a significant increase in the severe and collapse damage states. More significant effect was observed in the thin-walled structure with increments of 76%, 80%, 71%, and 68% in the intensity measure at which the 50% of exceedance probability for slight, moderate, extensive, and collapse damage states, respectively is reached. Furthermore, the steep slope observed in the fragility curve for the slight damage state, when considering the SSI, clearly indicates that the assessed building is highly

susceptible to experiencing slight damage even at low intensity levels. These results show that neglecting SSI in fragility analyses underestimates the vulnerability of the buildings.

5   Perspectives and Recommendations

The findings of this study underscore the effect that the SSI exerts in the seismic performance of two different buildings founded on soft soils of Bogotá. To extend the findings of this study, future works could investigate the seismic performance of tall and low buildings delving into the thin walls structural system since it showed to be the more susceptible to the inclusion of the SSI. Additionally, other SSI modeling approaches can be pursued (i.e., the direct approach) or different materials to those used for this research.

The author recommendations regarding the SSI modeling consists of an appropriate selection of the soil parameters, especially when the nonlinear condition of the soil is considered. Additionally, when evaluating the dynamic response of the buildings an appropriate selection of the ground motion records should be addressed considering the site seismic hazard.

6   References

[1]   C. Jian, B. Guobin, Y. Chun, C. Qingjun, and Z. Zhiliang, "Calculation Methods for Inter-Story Drifts of Building Structures," *Advances in Structural Engineering*, vol. 5, pp. 735–745, 2014.

[2]   P. R. Ranjbar and H. Naderpour, "Probabilistic evaluation of seismic resilience for typical vital buildings in terms of vulnerability curves," *Structures*, vol. 23, pp. 314–323, Feb. 2020, doi: 10.1016/j.istruc.2019.10.017.

[3]   A. G. Tyapin, *Soil-structure Interaction in Seismic Analysis*. 2019.

[4]   Y. Ohsaki, "Niigata Earthquakes, 1964 Building Damage and Soil Condition," *Soil and Foundation*, vol. VII, no. 2, pp. 14–37, 1966.

[5]   M. P. Romo, "Clay Behavior, Ground Response and Soil-Structure Interaction Studies in Mexico City Studies in Mexico City," in *Third Internation Conference on Recent Advances in Geotechnical Earthquake Engineering and Soil Dynamics*, 1995. [Online]. Available: https://scholarsmine.mst.edu/icrageesd/03icrageesd/session16/8

[6]   P. A. Marín, M. M. Suárez, and S. López, "Interacción Dinámica Suelo-Estructura Aplicada a Distintas Geometrías de Cimentación (Vibración Transmitida del Suelo a la Estructura)," México, 2016.

[7]   G. Savaris, P. H. Hallak, and P. C. A. Maia, "Understanding the Mechanism of Static Soil-Structure Interaction-A Case Study," *Soils and Rocks*, vol. 34, no. 3, pp. 195–206, Dec. 2011.

[8]   H. Asadi-Ghoozhdi and R. Attarnejad, "A Winkler-based model for inelastic response of soil–structure systems with embedded foundation considering kinematic and inertial interaction effects," *Structures*, vol. 28, pp. 589–603, Dec. 2020, doi: 10.1016/J.ISTRUC.2020.09.009.

[9]   Federal Emergency Management Agency, "FEMA P-2091, A Practical Guide to Soil-Structure Interaction," 2020. [Online]. Available: www.ATCouncil.org

[10] NEHRP, "Selecting and Scaling Earthquake Ground Motions for Performing Response-History Analyses," 2011.

[11] E. Kausel and M. Irfan Baig, "Laplace transform of products of Bessel functions: A visitation of earlier formulas," *Q Appl Math*, vol. 70, no. 1, pp. 77–97, Sep. 2011, doi: 10.1090/s0033-569x-2011-01239-2.

[12] J. Dominguez and J. M. Roesset, "Dynamic stiffness of rectangular foundations," Aug. 1978.

[13] S. Kleiven, P. Halldin, and D. Zenkert, "Dynamic Finite Element Methods," Stockholm, 2001.

[14] M. Novak, "Scholars' Mine Scholars' Mine Piles Under Dynamic Loads Piles Under Dynamic Loads Piles Under Dynamic Loads," in *Second International Conference on Recent Advances in Geotechnical Earthquake Engineering and Soli Dynamics*, 1991. [Online]. Available: https://scholarsmine.mst.edu/icrageesd/02icrageesd/session14/12

[15] B. Bapir, L. Abrahamczyk, T. Wichtmann, and L. F. Prada-Sarmiento, "Soil-structure interaction: A state-of-the-art review of modeling techniques and studies on seismic

response of building structures," *Frontiers in Built Environment*, vol. 9. Frontiers Media S.A., Feb. 03, 2023. doi: 10.3389/fbuil.2023.1120351.

[16] V. Anand and S. R. Satish Kumar, "Seismic Soil-structure Interaction: A State-of-the-Art Review," *Structures*, vol. 16. Elsevier Ltd, pp. 317–326, Nov. 01, 2018. doi: 10.1016/j.istruc.2018.10.009.

[17] R. W. Boulanger, C. J. Curras, B. L. Kutter, D. W. Wilson, and A. Abghari, "Seismic Soil-Pile-Structure Interaction Experiments and Analyses," 1999.

[18] G. Gazetas, *Foundation Engineering Handbook*. New York, 1991.

[19] J. E. Bowles, *Foundation analysis and design*. McGraw-Hill, 1996.

[20] E. D. Booth, J. W. Pappin, J. H. Mills, M. R. Degg, and R. S. Steedman, "The Mexican Earthquake of 19th September 1985," England, Sep. 1986.

[21] L. E. Pérez-Rocha and J. Avilés, "Evaluación de Efectos de Interacción en Resistencias Inelásticas," *Revista de Ingeniería Sísmica*, vol. 69, pp. 45–71, 2003.

[22] J. Avilés and L. E. Pérez-Rocha, "Bases para las Nuevas Disposiciones Reglamentarias Sobre Interacción Dinámica Suelo-Estructura," *Revista de Ingeniería Sísmica No*, vol. 71, pp. 1–36, 2004.

[23] J. Avilés and L. E. Pérez-Rocha, "Design concepts for yielding structures on flexible foundation," *Eng Struct*, vol. 27, no. 3, pp. 443–454, Feb. 2005, doi: 10.1016/j.engstruct.2004.11.005.

[24]   A. Bárcena and L. Esteva, "Influence of dynamic soil-structure interaction on the nonlinear response and seismic reliability of multistorey systems," *Earthq Eng Struct Dyn*, vol. 36, no. 3, pp. 327–346, 2007, doi: 10.1002/eqe.633.

[25]   L. R. Fernández Sola and J. Avilés López, "Efectos de Interacción Suelo-Estructura en Edificios con Planta Baja Blanda," *Revista de Ingeniería Sísmica*, vol. 79, pp. 71–90, 2008.

[26]   J. Avilés and L. E. Pérez-Rocha, "Effects of foundation embedment during building-soil interaction," *Earthq Eng Struct Dyn*, vol. 27, no. 12, pp. 1523–1540, Dec. 1998, doi: 10.1002/(SICI)1096-9845(199812)27:12<1523::AID-EQE798>3.0.CO;2-5.

[27]   INGEOMINAS and Universidad de Los Andes, "Microzonificacion sismica de santa fe de bogota," 1997.

[28]   A. B. Acevedo *et al.*, "Seismic risk assessment for the residential buildings of the major three cities in Colombia: Bogotá, Medellín, and Cali," *Earthquake Spectra*, vol. 36, no. 1_suppl, pp. 298–320, Oct. 2020, doi: 10.1177/8755293020942537.

[29]   M. Villar-Vega *et al.*, "Development of a Fragility Model for the Residential Building Stock in South America," 2017.

[30]   H. Melendez and E. Santisteban, "Enaluación de la Vulnerabilidad Sísmica del Hospital San Ignacio y su Rehabilitación Basados en Curvas de Fragilidad," Pontificia Universidad Javeriana, Bogotá, 2014.

[31]   O. Arroyo, D. Feliciano, J. Carrillo, and M. A. Hube, "Seismic performance of mid-rise thin concrete wall buildings lightly reinforced with deformed bars or welded wire mesh," *Eng Struct*, vol. 241, Aug. 2021, doi: 10.1016/j.engstruct.2021.112455.

[32] N. Bahamon, "Análisis de Interacción Suelo Estructura en Conjunto con un Análisis PushOver en una Edificación de 10 Pisos en Pórticos de Concreto, en Zonas Lacustres de la Microzonificación Sísmica de Bogotá," Universidad Miliar Nueva Granada, Bogotá, 2018.

[33] Fondo de Prevención y Atención de Emergencia, "Zonificación sísmica de Bogotá para el diseño sismo resistente de edificaciones," Bogotá, 2010.

[34] J. P. Stewart, R. B. Seed, and G. L. Fenves, "Seismic Soil-Structure Interaction in Buildings. II: Empirical Findings," *Journal of Geotechnical and Geoenvironmental Engineering*, vol. 125, no. 1, pp. 38–48, Jan. 1999, doi: 10.1061/(ASCE)1090-0241(1999)125:1(38).

[35] G. Mylonakis and G. Gazetas, "Seismic soil-structure interaction: Beneficial or detrimental?," *Journal of Earthquake Engineering*, vol. 4, no. 3, pp. 277–301, 2000, doi: 10.1080/13632460009350372.

[36] S. Soltani-Azar, "Evaluation of the Seismic Response of Reinforced Concrete Buildings Based on Time-History Analysis considering Nonlinear Soil Effects," *Journal of Earthquake Engineering*, vol. 27, no. 7, pp. 1690–1710, 2023, doi: 10.1080/13632469.2022.2087795.

[37] S. Bandyopadhyay, Y. M. Parulekar, and A. Sengupta, "MSA-based seismic fragility analysis of RC structures considering soil nonlinearity effects and time histories compatible to uniform hazard spectra," *Structures*, vol. 54, pp. 330–347, Aug. 2023, doi: 10.1016/j.istruc.2023.05.076.

[38] I. Kraus and D. Džakić, "Soil-structure interaction effects on seismic behaviour of reinforced concrete frames," in *International Conference on Earthquake Engineering* , Skopje, 2013.

[39] A. Bakhshi and M. Ansari, "Development of seismic fragility curves for reinforced concrete tall buildings," in *Proceedings of the International Conference on Structural Dynamic* , *EURODYN*, 2014.

[40] M. R. Akhoondi and F. Behnamfar, "Seismic fragility curves of steel structures including soil-structure interaction and variation of soil parameters," *Soil Dynamics and Earthquake Engineering*, vol. 143, Apr. 2021, doi: 10.1016/j.soildyn.2021.106609.

[41] A. Anvarsamarin, F. R. Rofooei, and M. Nekooei, "Soil-Structure Interaction Effect on Fragility Curve of 3D Models of Concrete Moment-Resisting Buildings," *Shock and Vibration*, vol. 2018, 2018, doi: 10.1155/2018/7270137.

[42] I. Oz, S. M. Senel, M. Palanci, and A. Kalkan, "Effect of soil-structure interaction on the seismic response of existing low and mid-rise RC buildings," *Applied Sciences (Switzerland)*, vol. 10, no. 23, pp. 1–21, Dec. 2020, doi: 10.3390/app10238357.

[43] H. Tahghighi and A. Mohammadi, "Numerical Evaluation of Soil-Structure Interaction Effects on the Seismic Performance and Vulnerability of Reinforced Concrete Buildings," *International Journal of Geomechanics*, vol. 20, no. 6, 2020, doi: 10.1061/(ASCE)GM.1943-5622.0001651.

[44] D. Pitilakis and C. Petridis, "Fragility curves for existing reinforced concrete buildings, including soil–structure interaction and site amplification effects," *Eng Struct*, vol. 269, Oct. 2022, doi: 10.1016/j.engstruct.2022.114733.

[45] M. V. Requena-Garcia-Cruz, R. Bento, P. Durand-Neyra, and A. Morales-Esteban, "Analysis of the soil structure-interaction effects on the seismic vulnerability of mid-rise RC buildings in Lisbon," *Structures*, vol. 38, pp. 599–617, Apr. 2022, doi: 10.1016/j.istruc.2022.02.024.

[46] S. Kechidi, A. Colaço, P. Alves Costa, J. M. Castro, and M. Marques, "Modelling of soil-structure interaction in OpenSees: A practical approach for performance-based seismic design," *Structures*, vol. 30, pp. 75–88, Apr. 2021, doi: 10.1016/j.istruc.2021.01.006.

[47] S. Carbonari, F. Dezi, and G. Leoni, "Nonlinear seismic behaviour of wall-frame dual systems accounting for soil-structure interaction," *Earthq Eng Struct Dyn*, vol. 41, no. 12, pp. 1651–1672, Oct. 2012, doi: 10.1002/eqe.1195.

[48] S. Carbonari, F. Dezi, and G. Leoni, "Linear soil-structure interaction of coupled wall-frame structures on pile foundations," *Soil Dynamics and Earthquake Engineering*, vol. 31, no. 9, pp. 1296–1309, Sep. 2011, doi: 10.1016/j.soildyn.2011.05.008.

[49] F. Mckenna, M. H. Scott, and G. L. Fenves, "Nonlinear Finite-Element Analysis Software Architecture Using Object Composition," *Journal of Computing in Civil Engineering*, vol. 24, pp. 95–107, 2010, doi: 10.1061/ASCECP.1943-5487.0000002.

[50] J. P. Wolf, *Foundation Vibration Analysis Using Simple Physical Models*. 1994. Accessed: Jun. 11, 2023. [Online]. Available: https://books.google.com.co/books?hl=es&lr=&id=fjF-dMkSs18C&oi=fnd&pg=PT24&ots=g_4YmvOI89&sig=i5qZkEeo_V6A2ywgo8WQennf vmg&redir_esc=y#v=onepage&q&f=false

[51] Servicio Geológico Colombiano, *Modelo Nacional de Amenaza Sísmica para Colombia*. Servicio Geológico Colombiano, 2020. doi: 10.32685/9789585279469.

[52] J. W. Chavez, "Overview of the Current Seismic Codes in Central and South America," *Bulletin of IISEE*, vol. 46, pp. 153–160, 2012.

[53] A. Ghobarah, "Seismic assessment of existing RC structures Seismic behaviour of end-plate connections View project," *Progress in Structural Engineering and Materials*, vol. 2, pp. 60–71, 2000, doi: 10.1002/(SICI)1528-2716(200001/03)2:13.0.CO;2-O.

[54] S. Cutcliffe, "On shaky ground: A history of earthquake resistant building design codes and safety standards in the United States in the twentieth century," *Bull Sci Technol Soc*, vol. 16, no. 6, pp. 311–327, 1996.

[55] S. Cutcliffe, "Earthquake resistant building design codes and safety standards: The California experience," *GeoJournal*, vol. 51, pp. 259–262, 2000.

[56] D. Contreras, "Popayán, the white city in Colombia, 35 years after the earthquake," 2018, doi: 10.13140/RG.2.2.23633.99687.

[57] O. Cardona, G. Wilches-Chaux, X. García, E. Mansilla, F. Ramírez, and M. Marulanda, "Estudio Sobre Desastres Ocurridos En Colombia: Estimación de Pérdidas y Cuantificación de Costos," 2004.

[58] AIS, "Normas Colombianas de Diseño y Construcción Sismo Resistente," 1998.

[59] AIS, "Reglamento Colombiano de Construcción Sismo Resistente," 2010.

[60] L. E. García, "Desarrollo de la normativa sismo resistente colombiana en los 30 años desde su primera expedición 1," *Revista de Ingeniería*, no. 41, pp. 71–77, Jul. 2014, doi: 10.16924/riua.v0i41.785.

[61] I. Iervolino, "What seismic risk do we design for when we design buildings?," in *Geotechnical, Geological and Earthquake Engineering*, vol. 46, Springer Netherlands, 2018, pp. 583–602. doi: 10.1007/978-3-319-75741-4_25.

[62] S. H. Jeong, A. M. Mwafy, and A. S. Elnashai, "Probabilistic seismic performance assessment of code-compliant multi-story RC buildings," *Eng Struct*, vol. 34, pp. 527–537, Jan. 2012, doi: 10.1016/j.engstruct.2011.10.019.

[63] N. L. Sinković, M. Brozovič, and M. Dolšek, "Risk-based seismic design for collapse safety," *Earthq Eng Struct Dyn*, vol. 45, no. 9, pp. 1451–1471, Jul. 2016, doi: 10.1002/eqe.2717.

[64] J. Carrillo, A. Rubiano, J. Carrillo, J. Blandón-Valencia, and A. Rubiano, "A review of conceptual transparency in US and Colombian seismic design building codes.," *Ingeniería e Investigación*, vol. 33, no. 2, pp. 24–29, 2014, [Online]. Available: https://www.researchgate.net/publication/255908669

[65] CEN, "Eurocode 8, design of structures for earthquake resistance," British Standards Institution, 2004. [Online]. Available: https://eurocodes.jrc.ec.europa.eu/EN-Eurocodes/eurocode-8-design-structures-earthquake-resistance

[66] Ministerio delle Infrastruture e dei Transporti, *Norme tecniche per le costruzioni*. Italy, 2018.

[67] C. A. Goulet *et al.*, "Evaluation of the seismic performance of a code-conforming reinforced-concrete frame building - From seismic hazard to collapse safety and economic losses," *Earthq Eng Struct Dyn*, vol. 36, no. 13, pp. 1973–1997, Oct. 2007, doi: 10.1002/eqe.694.

[68] B. R. Ellingwood, O. C. Celik, and K. Kinali, "Fragility assessment of building structural systems in Mid-America," *Earthq Eng Struct Dyn*, vol. 36, no. 13, pp. 1935–1952, Oct. 2007, doi: 10.1002/eqe.693.

[69] C. A. Arteta *et al.*, "Response of mid-rise reinforced concrete frame buildings to the 2017 Puebla earthquake," *Earthquake Spectra*, vol. 35, no. 4. Earthquake Engineering Research Institute, pp. 1763–1793, 2019. doi: 10.1193/061218EQS144M.

[70] Y. E. Ibrahim and M. M. El-Shami, "Seismic fragility curves for mid-rise reinforced concrete frames in Kingdom of Saudi Arabia," *IES Journal Part A: Civil and Structural Engineering*, vol. 4, no. 4, pp. 213–223, Nov. 2011, doi: 10.1080/19373260.2011.609325.

[71] C. B. Haselton, A. B. Liel, G. G. Deierlein, B. S. Dean, and J. H. Chou, "Seismic Collapse Safety of Reinforced Concrete Buildings. I: Assessment of Ductile Moment Frames," *Journal of Structural Engineering*, vol. 137, no. 4, pp. 481–491, 2011, doi: 10.1061/(ASCE)ST.1943-541X.0000318.

[72] G. Camata *et al.*, "Rintc project: Nonlinear dynamic analyses of Italian code-conforming reinforced concrete buildings for risk of collapse assessment," in *6th International Conference on Computational Methods in Structural Dynamics and Earthquake Engineering*, National Technical University of Athens, 2017, pp. 1474–1485. doi: 10.7712/120117.5507.17050.

[73] L. Macedo and J. M. Castro, "Collapse performance assessment of steel moment frames designed to Eurocode 8," *Eng Fail Anal*, vol. 126, p. 105445, Aug. 2021, doi: 10.1016/j.engfailanal.2021.105445.

[74] NEHRP, "Evaluation of the FEMA P-695 Methodology for Quantification of Building Seismic Performance Factors," 2010.

[75] A. Suzuki and I. Iervolino, "Seismic Fragility of Code-conforming Italian Buildings Based on SDoF Approximation," *Journal of Earthquake Engineering*, vol. 25, pp. 2873–2907, 2021, doi: 10.1080/13632469.2019.1657989.

[76] CSI, "ETABS-Three-Dimensional Analysis of Building Systems, Users' Manual," *Computers and Structures Inc., Berkeley, California*, 1997.

[77] D. Vamvatsikos and C. A. Cornell, "Applied incremental dynamic analysis," *Earthquake Spectra*, vol. 20, no. 2, pp. 523–553, 2004, doi: 10.1193/1.1737737.

[78] DANE, "Censo Nacional de Población y Vivienda," www.dane.gov.co.

[79] DANE, "PIB por departamento," https://www.dane.gov.co/index.php/estadisticas-por-tema/cuentas-nacionales/cuentas-nacionales-departamentales.

[80] DANE, "Pobreza y Desigualdad," https://www.dane.gov.co/index.php/estadisticas-por-tema/pobreza-y-condiciones-de-vida/pobreza-monetaria.

[81] DANE, "Vivienda VIS y NO VIS - Históricos," https://www.dane.gov.co/index.php/estadisticas-por-tema/construccion/vivienda-vis-y-no-vis/vivienda-vis-y-no-vis.

[82] Servicio Geológico Colombiano, "Amenaza Sísmica."

[83] O. Arroyo, J. Barros, and L. Ramos, "Comparison of the reinforced-concrete seismic provisions of the design codes of the United States, Colombia, and Ecuador for low-rise

frames," *Earthquake Spectra*, vol. 34, no. 2, pp. 441–458, May 2018, doi: 10.1193/102116EQS178EP.

[84] ASTM, "Standard specification for low-alloy steel deformed and plain bars for concrete reinforcement.," *A706/A706M-09b*, 2009.

[85] A. Neuenhofer and F. C. Filippou, "Geometrically Nonlinear Flexibility-Based Frame Finite Element," *Journal of Structural Engineering*, vol. 124, no. 6, pp. 704–711, 1998.

[86] J. B. Mander, M. J. N. Priestley, and R. Park, "Theoretical Stress-Strain Model for Confined Concrete," *Journal of Structural Engineering*, vol. 114, no. 8, pp. 1804–1826, 1988.

[87] J. Coleman and E. Spacone, "Localization Issues in Force-Based Frame Elements," *Journal of Structural Engineering*, vol. 127, no. 11, pp. 1257–1265, Nov. 2001, doi: 10.1061/(asce)0733-9445(2001)127:11(1257).

[88] J. Carrillo, H. Lozano, and C. Arteta, "Mechanical properties of steel reinforcing bars for concrete structures in central Colombia," *Journal of Building Engineering*, vol. 33, Jan. 2021, doi: 10.1016/j.jobe.2020.101858.

[89] P. Taghvaei, "Evaluating the Functional Recovery Performance of Modern Residential Tall Reinforced Concrete Shear Wall Buildings in Metro Vancouver," 2019.

[90] M. A. Bakkar, R. Saha, and D. Das, "Low Cycle Fatigue Performance and Failure Analysis of Reinforcing Bar," *Metals and Materials International*, vol. 27, no. 12, pp. 4952–4966, Dec. 2021, doi: 10.1007/s12540-020-00839-x.

[91] M. Ajmal, "Seismic evaluation and retrofit assessment of multi storey structures using pushover analysis (POA)," Dhahran, 2012.

[92]   F. Khoshnoudian, S. Mestri, and F. Abedinik, "Proposal of lateral load pattern for pushover analysis of RC buildings," *Computational Methods in Civil Engineering*, vol. 2, no. 2, pp. 169–183, 2011, [Online]. Available: http://research.guilan.ac.ir/cmce

[93]   G. G. Deierlein, A. M. Reinhorn, and M. R. Willford, *Nonlinear Structural Analysis For Seismic Design: A Guide for Practicing Engineers*. NEHRP Seismic Design Technical Brief No. 1, 2010.

[94]   J. W. Baker, "Efficient analytical fragility function fitting using dynamic structural analysis," *Earthquake Spectra*, vol. 31, no. 1, pp. 579–599, Feb. 2015, doi: 10.1193/021113EQS025M.

[95]   D. Vamvatsikos and C. Allin Cornell, "Incremental dynamic analysis," *Earthq Eng Struct Dyn*, vol. 31, no. 3, pp. 491–514, 2002, doi: 10.1002/eqe.141.

[96]   PAHO, "Pan American Health Organization (PAHO)."

[97]   FEMA, "Earthquake-Resistant Design Concepts," Washington, D.C, 2010. [Online]. Available: www.bssconline.org

[98]   S. Karafagka, S. Fotopoulou, and D. Pitilakis, "Fragility curves of non-ductile RC frame buildings on saturated soils including liquefaction effects and soil–structure interaction," *Bulletin of Earthquake Engineering*, vol. 19, no. 15, pp. 6443–6468, Dec. 2021, doi: 10.1007/s10518-021-01081-5.

[99]   NIST, "Soil-Structure Interaction for Building Structures," Sep. 2012.

[100]   P. C. Jennings and J. Bielak, "Dynamics of Building-Soil Interaction," *Bulletin of tile Seismological Society of America*, vol. 63, no. 1, pp. 9–48, 1973.

[101] J. P. Wolf, "Soil-structure-interaction analysis in time domain," *Nuclear Engineering and Design*, vol. 111, no. 3, pp. 381–393, Feb. 1989, doi: 10.1016/0029-5493(89)90249-5.

[102] E. Tapia-Hernández, Y. De Jesús-Martínez, and L. F. Sola, "Dynamic soil-structure interaction of ductile steel frames in soft soils," *Advanced Steel Construction*, vol. 13, no. 4, pp. 361–377, 2017, doi: 10.18057/IJASC.2017.13.4.3.

[103] D. Forcellini, "Seismic fragility of tall buildings considering soil structure interaction (SSI) effects," *Structures*, vol. 45, pp. 999–1011, Nov. 2022, doi: 10.1016/j.istruc.2022.09.070.

[104] World Housing Encyclopedia, "RC Structural Wall Building." Accessed: Jun. 13, 2023. [Online]. Available: http://db.world-housing.net/building/109/

[105] J. Carrillo, E. Cubillos, and P. F. Parra, "Modeling the seismic response of thin concrete walls using the non-linear Beam-Truss Model," *Journal of Building Engineering*, vol. 52, p. 104424, Jul. 2022, doi: 10.1016/J.JOBE.2022.104424.

[106] L. G. Quiroz and Y. Maruyama, "Assessment of seismic performance of high-rise thin RC wall buildings in Lima, Peru using fragility functions," *Journal of Disaster Research*, vol. 9, no. 6, pp. 1026–1031, 2014, doi: 10.20965/jdr.2014.p1026.

[107] D. Ugalde and D. Lopez-Garcia, "Analysis of the seismic capacity of Chilean residential RC shear wall buildings," *Journal of Building Engineering*, vol. 31, Sep. 2020, doi: 10.1016/j.jobe.2020.101369.

[108] J. Velásquez, S. López, C. Rodríguez, and J. Acero, "Seismic damage assessment for thin-walled reinforced concrete buildings in urban areas in Peru," in *11th National Conference on Earthquake Engineering 2018, NCEE 2018: Integrating Science, Engineering, and Policy*, 2018, pp. 4083–4093.

[109] M. G. C. Santos and M. R. S. Corrêa, "Analysis of the effects of soil-structure interaction in reinforced concrete wall buildings on shallow foundation," *Revista IBRACON de Estruturas e Materiais*, vol. 11, no. 5, pp. 1076–1109, Oct. 2018, doi: 10.1590/s1983-41952018000500010.

[110] M. Á. Rodríguez Gutiérrez, C. Magna-Verdugo, and J. A. Abell, "Influence of Soil-Structure-Interaction in Shear-wall RC Buildings Fragility Curves," in *Eleventh U.S. National Conference on Earthquake Engineering*, 2018. [Online]. Available: https://www.researchgate.net/publication/326881587

[111] M. Juárez-Camarena, G. Auvinet-Guichard, and E. Méndez-Sánchez, "Geotechnical Zoning of Mexico Valley Subsoil," *Ingeniería, Investigación y Tecnología*, vol. 17, no. 3, pp. 297–308, Jul. 2016, doi: 10.1016/j.riit.2016.07.001.

[112] J. Avilés and L. E. Pérez-Rocha, "Use of global ductility for design of structure-foundation systems," *Soil Dynamics and Earthquake Engineering*, vol. 31, no. 7, pp. 1018–1026, Jul. 2011, doi: 10.1016/j.soildyn.2011.03.008.

[113] G. Díaz-Fañas, S. Nikolaou, O.-J. Ktenidou, E. Garini, G. Gazetas, and X. Ma, "Mexico City 1985 and 2017 Earthquakes: Soil Response and Code Lessons," in *Geotechnical Engineering in the XXI Century: Lessons learned and future challenges*, 2019, pp. 1991–2000. doi: 10.3233/STAL190259.

[114] World Housing Encyclopedia, "Ductile RC Frames." Accessed: Jun. 13, 2023. [Online]. Available: http://db.world-housing.net/building/201/

[115] K. Kolozvari, K. Orakcal, and J. W. Wallace, "New opensees models for simulating nonlinear flexural and coupled shear-flexural behavior of RC walls and columns," *Comput Struct*, vol. 196, pp. 246–262, Feb. 2018, doi: 10.1016/J.COMPSTRUC.2017.10.010.

[116] K. Terzaghi and R. B. Peck, *Mecánica de Suelos en la Ingeniería Práctica*, 2nd ed. EL ATENEO, 1973.

[117] H. G. Poulos and E. H. Davis, *Pile Foundation Analysis and Design_Poulos_Davis_1980*. 1980.

[118] J. B. Hansen, "A General Formula for Bearing Capacity," *Ingeniøren, International Edition*, vol. 5, pp. 38–46, 1961.

[119] R. G. McClarren, "Gauss Quadrature and Multi-dimensional Integrals," *Computational Nuclear Engineering and Radiological Science Using Python*, pp. 287–299, 2018, doi: 10.1016/B978-0-12-812253-2.00018-2.

[120] B. D. Scott, R. Park, and M. J. N. Priestley, "Stress-Strain Behavior of Concrete Confined by Overlapping Hoops at Low and High Strain Rates," *Journal Proceedings*, vol. 79, no. 1, pp. 13–27, Jan. 1982, doi: 10.14359/10875.

[121] L. Ramos and M. A. Hube, "Seismic response of reinforced concrete wall buildings with nonlinear coupling slabs," *Eng Struct*, vol. 234, May 2021, doi: 10.1016/j.engstruct.2021.111888.

[122] "Localization issues in force-based frame elements," *Journal of Structural Engineering*, vol. 127, no. 11, pp. 1257–1265, 2001.

[123] A. Toro, S. Ibarguen, A. R. Ortiz, and J. Carrillo, "Caracterización de la Incertidumbre Asociada a las Expresiones Usadas Para Estimar el Módulo de Elasticidad del Concreto

Producido en Colombia - Uncertainty Quantification for the Elastic Modulus of the Concrete Produced in Colombia," in *Jornadas XIX Geotécnicas, XXI Estructurales*, Aug. 2021.

[124] A. Vulcano, V. Bertero, and V. Colotti, "Analytical Modeling of R/C Structural Walls," in *Proceedings of Ninth World Conference on Earthquale Engineering*, Tokyo-Kyoto, Aug. 1988.

[125] J. Carrillo, C. Diaz, and C. A. Arteta, "Tensile mechanical properties of the electro-welded wire meshes available in Bogotá Colombia," *Constr Build Mater*, vol. 195, pp. 352–362, Jan. 2019, doi: 10.1016/j.conbuildmat.2018.11.096.

[126] J. Moehle, "Seismic Design of Reinforced Concrete Buildings, 2014," 2015.

[127] E. Winkler, *Die Lehre von der Elastizität und Festigkeit*. Prague, 1867. Accessed: Jun. 13, 2023. [Online]. Available: https://books.google.com.co/books?id=25E5AAAAcAAJ&redir_esc=y

[128] D. Z. Yankelevsky, M. Eisenberger, and M. A. Adin, "Analysis of Beams on Nonlinear Winkler Foundation," *Comput Struct*, vol. 31, no. 2, pp. 287–292, 1989.

[129] R. W. Boulanger, C. J. Curras, D. W. Wilson, and A. Abghari, "Appendix: Equations and Example Responses for the PySimple1 Material," 2003.

[130] R. W. Boulanger, C. J. Curras, D. W. Wilson, and A. Abghari, "Appendix: Equations and Example Responses for the TzSimple1 Material," 2003.

[131] R. W. Boulanger, C. J. Curras, D. W. Wilson, and A. Abghari, "Appendix: Equations and Example Responses for the QzSimple1 Material," 2003.

[132] H. Matlock, "Correlations for Design of Laterally Loaded Piles in Soft Clay," in *Offshore Technology Conference*, Texas, 1970.

[133] G. G. Meyerhof, "The Ultimate Bearing Capacity of Foundations on Slopes," in *4th ICSMFE*, London, 1957, pp. 384–386.

[134] C. Harden, "Numerical modeling of the nonlinear cyclic response of shallow foundations," University of California, 2005. [Online]. Available: https://www.researchgate.net/publication/35229284

[135] American Petroleum Institute (API), "API RPA 2: Recommended Practice for Planning, Designing and Constructing Fixed Offshore Platforms - Working Stress Design," Washington, D.C, 2010.

[136] M. Suarez, "Modelos de Comportamiento Dinámico para las Arcillas de Bogotá," Universidad de Los Andes, Bogotá, 2004.

[137] R. V. Whitman, "Earthquake Engineering," *Encyclopedia of Physical Science and Technology*, pp. 717–729, Jan. 2003, doi: 10.1016/B0-12-227410-5/00877-2.

[138] M. Paz and Y. H. Kim, "Structural Dynamics," 2019, doi: 10.1007/978-3-319-94743-3.

[139] C. A. Arteta and N. A. Abrahamson, "Conditional Scenario Spectra (CSS) for Hazard-Consistent Analysis of Engineering Systems," *https://doi.org/10.1193/102116EQS176M*, vol. 35, no. 2, pp. 737–757, May 2019, doi: 10.1193/102116EQS176M.

[140] Federal Emergency Management Agency (FEMA), "Hazus MH 2.1 Technical Manual," 2003. [Online]. Available: www.msc.fema.gov

[141] J. W. Baker, "Efficient analytical fragility function fitting using dynamic structural analysis," *Earthquake Spectra*, vol. 31, no. 1, pp. 579–599, Feb. 2015, doi: 10.1193/021113EQS025M.

[142] NEHRP, "Soil-Structure Interaction for Building Structures," 2012.

[143] L. Wang and T. Ishihara, "New p-y model for seismic loading prediction of pile foundations in non-liquefiable and liquefiable soils considering modulus reduction and damping curves," *Soils and Foundations*, vol. 62, no. 5, Oct. 2022, doi: 10.1016/J.SANDF.2022.101201.